

NASA-CR-174645

R84AEB378



National Aeronautics and Space Administration

EXTENDED PARAMETRIC REPRESENTATION OF COMPRESSOR FANS AND TURBINES

Volume I - CMGEN User's Manual

FINAL REPORT

March 1984

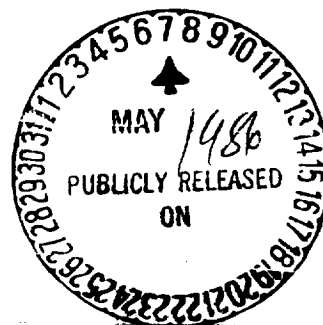
By

General Electric Company
Aircraft Engine Business Group
Advanced Technology Programs Dept.
Cincinnati, Ohio 45215



FOR

NATIONAL AERONAUTICS AND SPACE ADMINISTRATION
LEWIS RESEARCH CENTER
21000 BROOKPARK ROAD
CLEVELAND, OHIO 44135



(NASA-CF-174645) EXTENDED PARAMETRIC REPRESENTATION OF COMPRESSOR FANS AND TURBINES. VOLUME 1: CMGEN USER'S MANUAL
Final Report, Aug. 1982 - Oct. 1983 (General Electric Co.) 60 p HC A04/MF A01 CACL 13I G3/37

N86-23936

Unclas
06032


Contract
NAS3-23055



Aircraft Engine Business Group
Advanced Technology Programs Department
Cincinnati, Ohio 45215



**ORIGINAL PAGE IS
OF POOR QUALITY**

1. Report No NASA CR-174645	2. Government Accession No.	3. Recipient's Catalog No.	
4. Title and Subtitle Extended Parametric Representation of Compressor Fans and Turbines Vol. I - CMGEN User's Manual	5. Report Date March 1984		6. Performing Organization Code
	7. Author(s) G.L. Converse and R.G. Giffin		
9. Performing Organization Name and Address General Electric Company Aircraft Engine Business Group Cincinnati, Ohio 45215	8. Performing Organization Report No. R84AEB378		
	10. Work Unit No.		
12. Sponsoring Agency Name and Address National Aeronautics and Space Administration Washington, D.C. 20546	11. Contract or Grant No. NAS3-23055		
	13. Type of Report and Period Covered Contract Report August 1982 - October 1983		
14. Sponsoring Agency Code			
15. Supplementary Notes Project Manager, James W. Gauntner, Aerospace Engineer, NASA Lewis Research Center, Cleveland, Ohio			
16. Abstract A modeling technique for fans, boosters, and compressors has been developed which will enable the user to obtain consistent and rapid off-design performance from design point input. The fans and compressors are assumed to be multi-stage machines incorporating front variable stators. The boosters are assumed to be fixed geometry machines. The modeling technique has been incorporated into a time sharing program to facilitate its use. Because this report contains a description of the input output data, values of typical inputs, and example cases, it is suitable as a user's manual. This report is the first of a three volume set describing the parametric representation of compressors, fans, and turbines. The titles of the three volumes are given below: <div style="margin-left: 40px;"> (1) Volume I CMGEN USER's Manual (Parametric Compressor Generator) (2) Volume II PART USER's Manual (Parametric Turbine) (3) Volume III MODFAN USER's Manual (Parametric Modulating Flow Fan) </div>			
17. Key Words (Suggested by Author(s)) Parametric fan, boosters, compressors off-design performance axial flow		18. Distribution Statement 	
19. Security Classif (of this report) Unclassified	20. Security Classif (of this page) Unclassified	21. No. of Pages 56	22. Price*

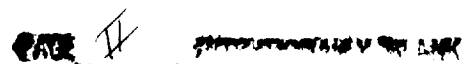
THE UNIVERSITY OF MICHIGAN LIBRARY

300 N ZEEB RD ANN ARBOR MI 48106-1099

TABLE OF CONTENTS

	<u>Page</u>
1.0 INTRODUCTION	1
2.0 PROGRAM STRUCTURE	5
3.0 PROGRAM INPUTS	7
4.0 PROGRAM OUTPUTS	13
5.0 PROGRAM DIAGNOSTICS	14
6.0 EXAMPLE CASES	16
7.0 ANALYTICAL BACKGROUND	27
7.1 Compressor Map Fitting System	27
7.1.1 Description of Current Compressor Map Fitting System	28
7.1.2 General Background	28
7.1.3 Compressor Efficiency Representation	32
7.1.4 Compressor Flow Representation	32
7.1.5 Compressor Base Curves	36
7.2 Discussion of the Derivation of the Parametric Curve Sets	38
LIST OF SYMBOLS	52
REFERENCES	53

PRECEDING PAGE BLANK NOT FILMED



LIST OF ILLUSTRATIONS

<u>Figure</u>		<u>Page</u>
1.	Typical Compressor Map (PR=12.0)	3
2.	Parametric Map Flow-Speed Relationship (LO T2 Schedule)	4
3.	Flow Chart Showing Flow of Control In CMGEN	6
4.	CMGEN Sample Terminal Conversation	10
5.	Parametric Booster Performance Map (PR=2.45)	12
6.	Dimensionless Compressor Performance Parameters	30
7.	Compressor Stage Characteristic	31
8.	Compressor Loss Representation.	33
9.	Stage Efficiency and Loss Characteristics	34
10.	Compressor Flow Representation	35
11.	Speed Line Sketch	37
12.	Variation of Backbone Flow Coefficient With Speed and Design Pressure Ratio	40
13.	Variation of Corrected Flow with Speed and Design Point Specific Flow (PR=12)	41
14.	Min-Loss Throttle Coefficient	42
15.	Min-Loss Efficiency Distribution	43
16.	Design Point Efficiency Variation with Pressure Ratio	44
17.	Variation of Loss Slope with Flow Coefficient	45
18.	Variation of Mach Number Slope with Speed	46

LIST OF ILLUSTRATIONS - (CONTINUED)

<u>Figure</u>		<u>Page</u>
19.	Variation of Mach Number Intercept with Speed and Design Pressure Ratio	47
20.	Bivariate Loss Curves	48
21.	Bivariate Flow Curves	49
22.	Flow Variation for HI T2 Schedule	50
23.	Parametric Map Flow-Speed Relationship (HI T2 Schedule)	51

LIST OF TABLES

<u>Table</u>		<u>Page</u>
1	Default Settings for Variables in NAMELIST "INPUT"	9

1.0 INTRODUCTION

The NASA Lewis Research Center employs a general computer program, NNEP, (Reference 1) for calculating the thermodynamic performance of jet propulsion engines. To calculate off-design engine performance, the user of NNEP must input component maps defining the characteristics of the various components over their full range of operating conditions.

For early cycle analysis of advanced propulsion systems, these map characteristics are not generally known because the geometry of the component has not been specified. Furthermore, the typical user of the program is not sufficiently knowledgeable and/or cannot afford the time to do an extensive design followed by an off-design analysis of the component in question to define the map characteristics. Typically, in this early stage, the user scales some available map.

The available methods for scaling maps can lead to significant errors in component representations. A traditional method of scaling a compressor map retains the flow speed relation of the base map and applies a constant pressure rise scalar calculated at the design point. Direct scaling of flow size is frequently used. The accuracy of such a procedure can be considerably improved by using parametrically generated component maps. A parametric component representation can be a scaling procedure which uses the key design point parameters to impace the fundamental differences in the map characteristics when generating the component maps.

The subject of this report is the parametric multistage compressor/fan program. The key design point parameters in the CMGEN program are:

1. Pressure ratio
2. Inlet corrected flow per unit area (i.e., inlet Mach Number).
3. Stall margin.

A 12 to 1 pressure ratio map generated by the program CMGEN is shown in Figure 1. A series of maps having different design point pressure ratios but identical inlet specific flows was also generated. The lapse rate (i.e., the flow speed variation) was then plotted along the peak efficiency ridge. Figure 2 shows the effect of design point pressure ratio on lapse rate. The variation in the flow speed with design pressure ratio is due to compressibility and associated mis-matching.

The above discussion illustrates the importance of having changes in design point parameters reflected by corresponding changes in the off-design characteristics of the performance maps. The more complete the parametric system (i.e., the more design point parameters it includes) the closer the calculated off-design performance representation can be to the actual performance.

The computer program CMGEN is an improved method for representing the off-design characteristics of the compression components when performing off-design performance calculations for advanced air-breathing jet engines. It is applicable to multi-stage fans and compressors having variable stators as well as fixed geometry boosters. It can be applied at any level of inlet corrected flow size.

The program uses design point data and semi-empirical correlations as input to generate off-design values of corrected flow, efficiency, and pressure ratio over a range of corrected speeds and pressure ratio parameters specified by the user.

The computer program CMGEN is compatible in both form and format with the cycle program of Reference 1, and the example map representation of Reference 2.

This report contains a description of the input-output data, values of typical inputs, and sample cases, it is suitable as a user's manual. A description giving the background of the engineering analysis used to generate the program is given near the end of the report.

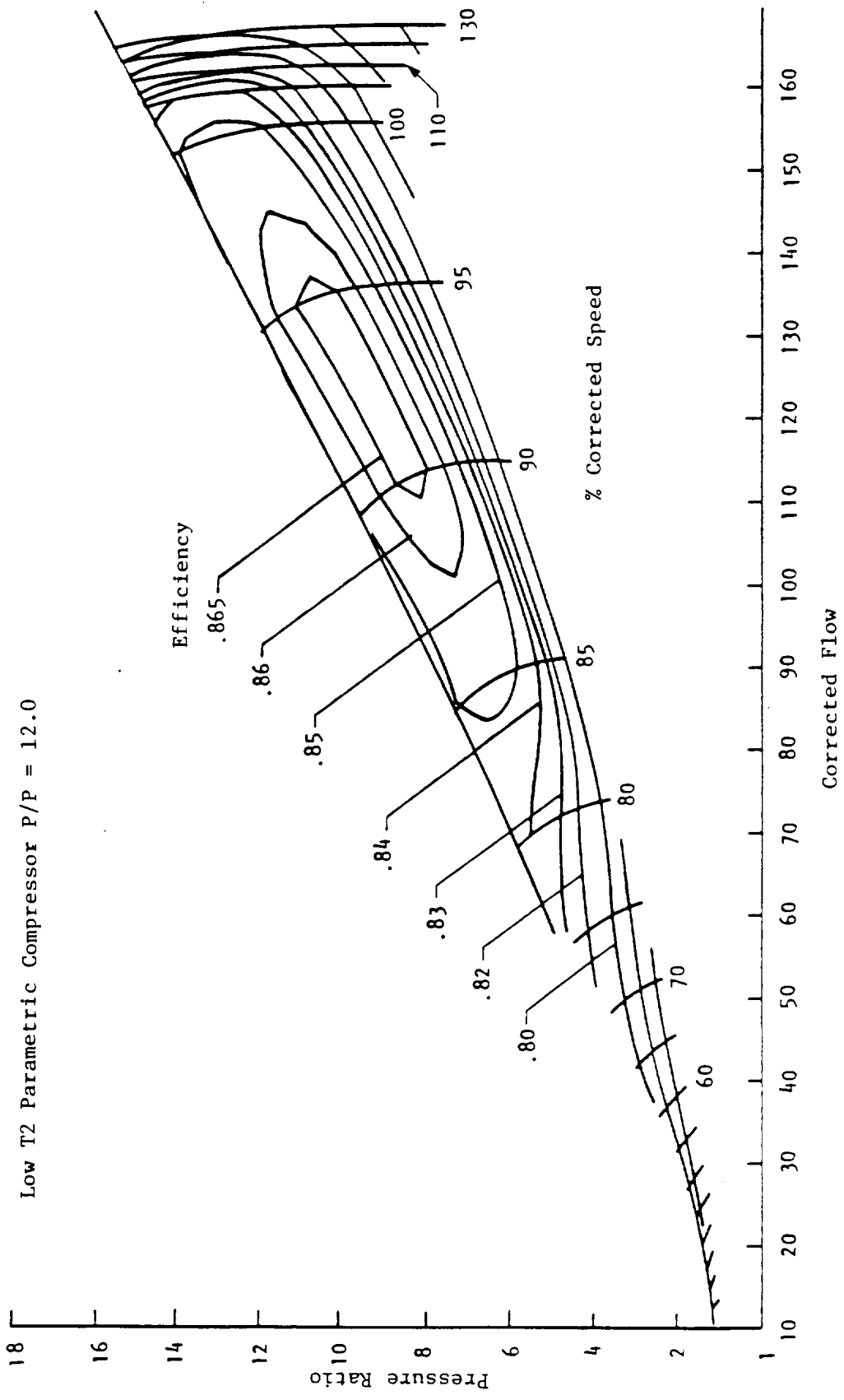


Figure 1. Typical Compressor Map.

ORIGINAL PAGE IS
OF POOR QUALITY

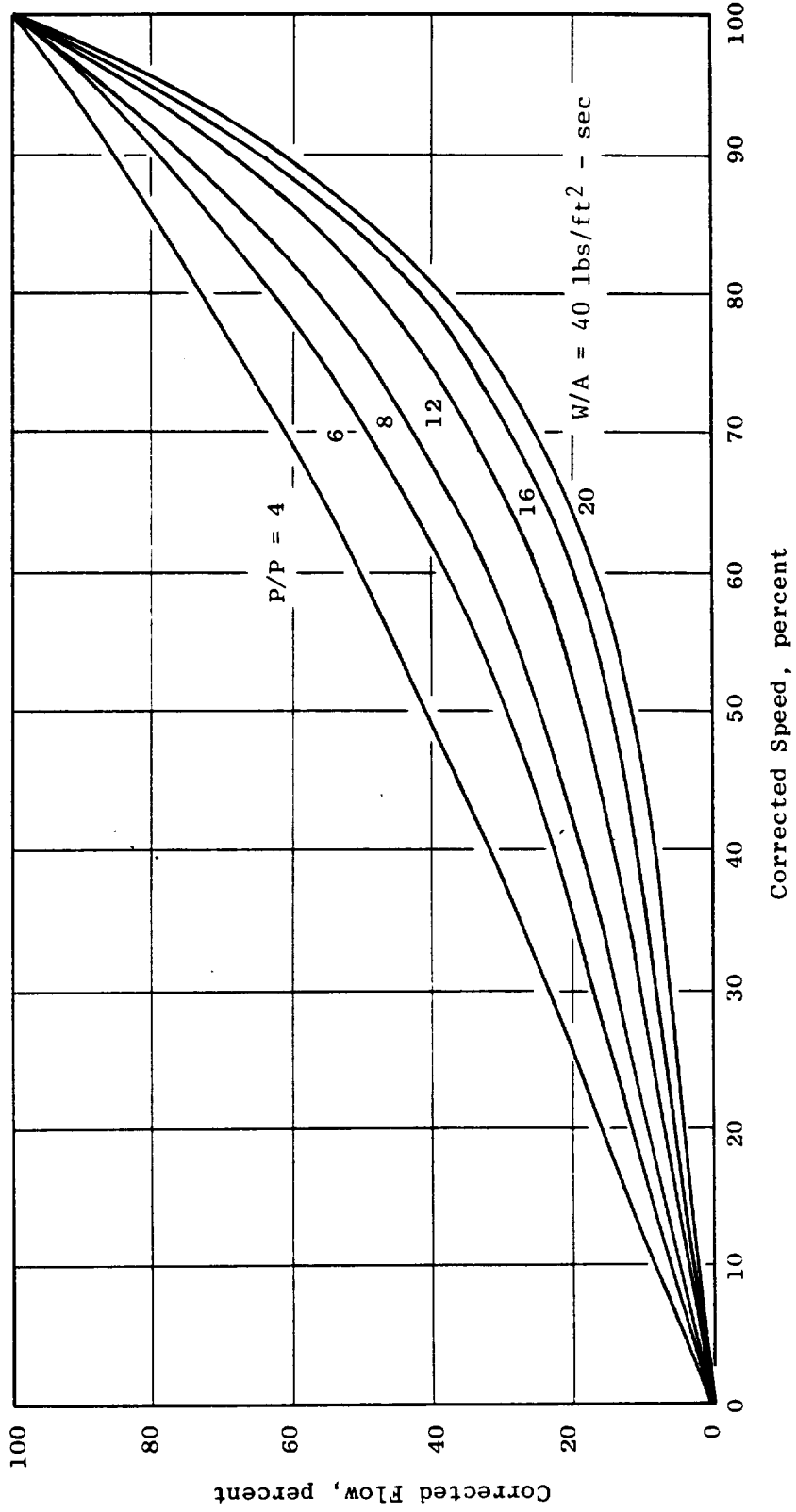


Figure 2. Parametric Map Flow-Speed Relationship (LO T2 Schedule).

2.0 PROGRAM STRUCTURE

A flow chart showing the flow of control in the computer program CMGEN (Compressor generator) is shown in Figure 3. After the input has been read and processed, the program reads in the set of component base curves selected by the user's setting of the ITYPE switch. These base curves are in NAMELIST form and reside on three external files. The program next carries out a design point calculation in which a number of additional design point values are calculated from the input values. The off-design calculation is then carried out for each value of corrected speed and R selected by the user. This calculation is carried out in the evaluation routine CPMXX. Finally, the output is written on three files plus an additional output file (File 22) which contains the five base curves discussed in Section 7.1.

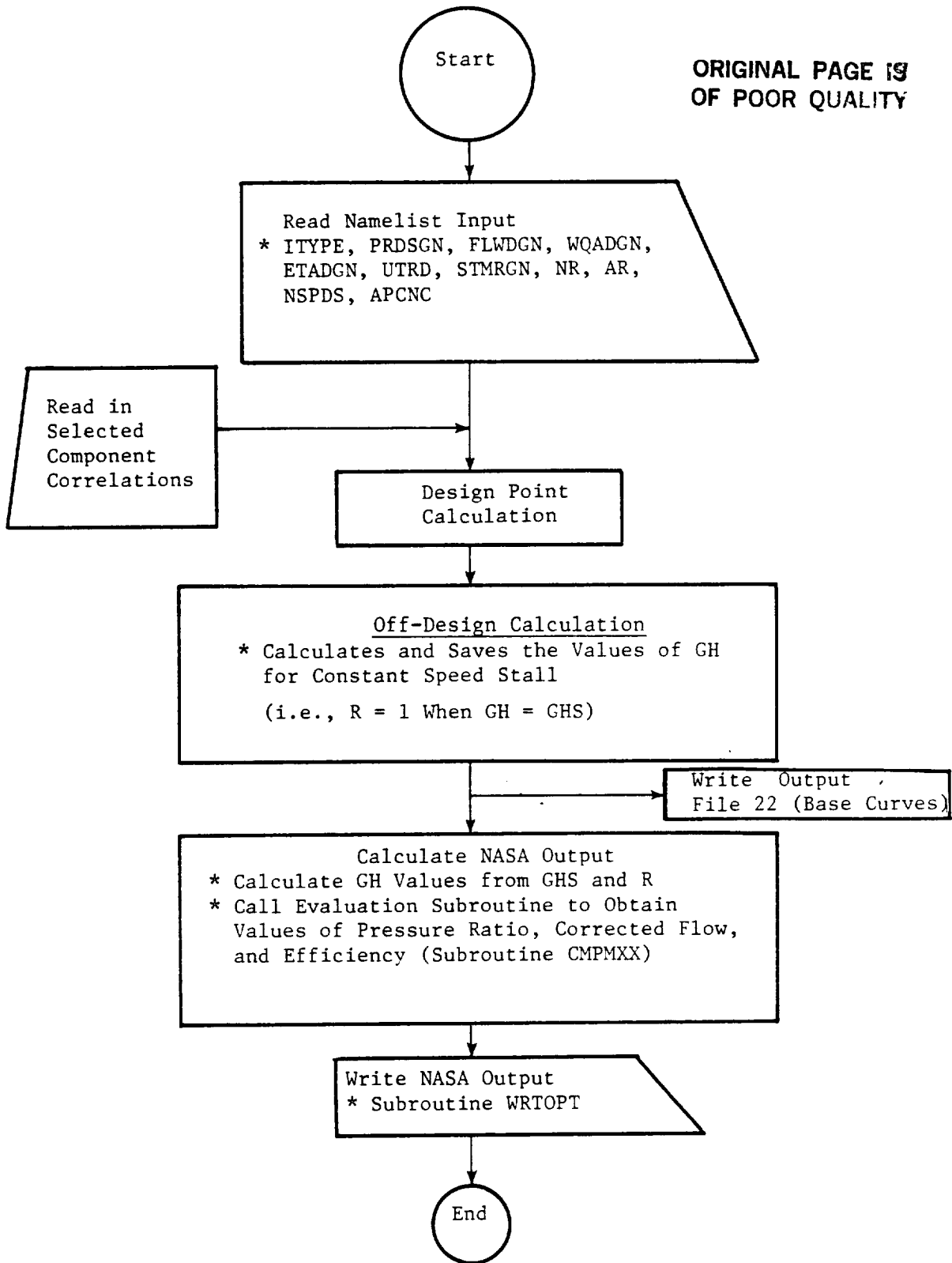


Figure 3. Flow Chart Showing Flow of Control in GMGEN.

3.0 PROGRAM INPUTS

All of the CMGEN inputs are of the free-field format (NAMELIST) type, and begin in Column two. There is no specified order to the inputs. The program first gives a brief description of the variables used in the NAMELIST INPUT. The default settings of these variables are then displayed. The user can then enter any changes in the design point values and/or the speed and R arrays. If the user wishes the program to generate a value for the design point efficiency, a zero value should be entered for ETADGN. The program will echo the updated NAMELIST values, then go into execution. Upon completion, the program will display a message to the effect that the NASA output files have been written on file codes 30, 31, and 32. File 22, which is also generated by the program, contains the component base curves which are discussed in section 7.1.

The input variables together with their default settings are listed in TABLE 1.

The first input variable in TABLE 1, ITYPE, is used to determine the type of component desired. The booster is assumed to be a multi-stage fixed geometry machine. Both the fan and compressor are assumed to be multi-stage machines having variable stators. Two sets of flow speed characteristics are generated by the program, a high T2 open stator schedule and a low T2 nominal stator schedule.

The range of design point pressure ratios applicable to each type of is as follows:

ITYPE	Component Type	Pressure Ratio Range	Variable Stator Schedule
1	Fan	2-5	High T2 & Low T2
2	Booster (fixed geometry)	1.2-5	None
3	Core Compressor	4-24	High T2 & Low T2

The next five variables in Table 1 set the key design point parameters. The program will calculate a design point efficiency. A flow size correction is included in the program. The flow size correction was obtained by using the results of a study in which a series of machines differing only in flow size were designed. The efficiency

correction is, therefore, an overall correction accounting for all flow sizes effects such as Reynold's number, tip clearance, tolerances, etc.

The last four variables in Table 1 are used to control the number of values of R and speed to be written on the output file. The R values are used to fix a point on a speed line. The R value is unity on the stall line and increases along a constant speed line as the flow increases. The algorithm used in CMGEN forces a value of R equal to two at the min-loss point which is slightly below the peak efficiency on the speed line. The concept of min-loss is discussed in section seven (7).

For example, in the input shown in Figure 4, all of the design point variables have been changed as well as the corrected speed array. The booster map which results is shown in Figure 5. The locus of the R=1 and 2 lines have been indicated on figure 5.

TABLE 1. DEFAULT SETTINGS FOR VARIABLE :
 NAMELIST "INPUT"

VARIABLE NAME	UNITS	DEFAULT VALUES	DESCRIPTION
ITYPE	NONE	3	Type of Component 1=Fan, 2=Booster, 3=Compressor
PRDSGN	NONE	12.0	Design point pressure ratio
FLWDGN	pps	155.0	Design point corrected flow
WQADGN	pps/ft ²	40.0	Design point corrected flow per unit annulus area
UTRD	fps	1000.0	Design point corrected first stage rotor tip speed
STMRGN	percent	15.0	Design point constant speed stall margin
NR		11	No. of R values
AR	NONE	1.,1.2,1.4, 1.6,1.8,2.0, 2.2,2.4,2.6, 2.8,3.0	Array of R values
NSPDS		12	No. of corrected speeds
APCNC	NONE	.1,.2,.3,.4, .5,.6,.7,.8, .9,1.0,1.1, 1.2	Array of corrected speeds

ORIGINAL PAGE IS
OF POOR QUALITY

PARAMETRIC FAN, BOOSTER, AND COMPRESSOR GENERATOR

VARIABLE NAMES USED IN NAMELIST INPUT

NAME	DESCRIPTION
ITYPE	COMP TYPE: 1=FAN, 2=BOOSTER, 3=COMPRESSOR
PROSGN	DESIGN POINT VALUE OF:
FLWDCN	PRESSURE RATIO
WQADGN	CORRECTED FLOW
ETADGN	CORRECTED FLOW PER UNIT ANNULUS AREA
UTRD	EFFICIENCY
STMRGN	CORRECTED FIRST STAGE ROTOR TIP SPEED
	CONSTANT SPEED STALL MARGIN
NR	NO OF R VALUES
AR	ARRAY OF R VALUES
NSPDS	NO OF CORRECTED SPEEDS
APCNC	ARRAY OF CORRECTED SPEEDS

```

NAMELIST          INPUT
ITYPE=           3
PROSGN=          12.000000,          FLWDCN=          155.000000
WQADGN=          40.000000,          ETADGN=           0.861000
UTRD =           1000.000000,        STMRGN=           16.000000
NSPDS =           12,
APCNC (I)=
  1             0.100000,             0.200000,             0.300000,             0.400000,
  5             0.500000,             0.600000,             0.700000,             0.800000,
  9             0.900000,             1.000000,             1.100000,             1.200000,
 13            1.300000,             1.300000,             1.300000,
NR =             11,
AR (I)=
  1             1.000000,             1.200000,             1.400000,             1.600000,
  5             1.800000,             2.000000,             2.200000,             2.400000,
  9             2.600000,             2.800000,             3.000000,             3.200000,
 13            3.200000,             3.200000,             3.200000,

```

```

END NAMELIST
ENTER CHANGES TO NAMELIST INPUT
-SINPUT ITYPE=2,PROSGN=2.45,FLWDCN=100.0,WQADGN=33.7,
-ETADGN=0.8,UTRD=869.7,STMRGN=14.34.
-NSPDS/APCNC=.359,.528,.661,.791,.88,.952,1.0,1.028,1.1448

```

```

NAMELIST          INPUT
ITYPE=           2
PROSGN=          2.450000,          FLWDCN=          100.000000
WQADGN=          33.700000,          ETADGN=           0.870754
UTRD =           869.699997,        STMRGN=           14.340000
NSPDS =           9,
APCNC (I)=
  1             0.359000,             0.528000,             0.661000,             0.791000,
  5             0.880000,             0.952000,             1.000000,             1.028000,
  9             1.144000,             1.000000,             1.100000,             1.200000,
 13            1.300000,             1.300000,             1.300000,
NR =             11,
AR (I)=
  1             1.000000,             1.200000,             1.400000,             1.600000,

```

Figure 4. CMGEN Sample Terminal Conversation.

ORIGINAL DATA
OF POOR QUALITY

```
      5      1.800000,      2.000000,      2.200000,      2.400000,
      9      2.600000,      2.800000,      3.000000,      3.200000,
     13      3.200000,      3.200000,      3.200000,
END      NAMELIST
MAP FILE ON TEMP FILE      22
YOU HAVE CREATED TEMP FILE      22
NASA OUTPUT ON FILE CODES 30,31,AND 32 &
```

Figure 4. CMGEN Sample Terminal Conversation (Continued).

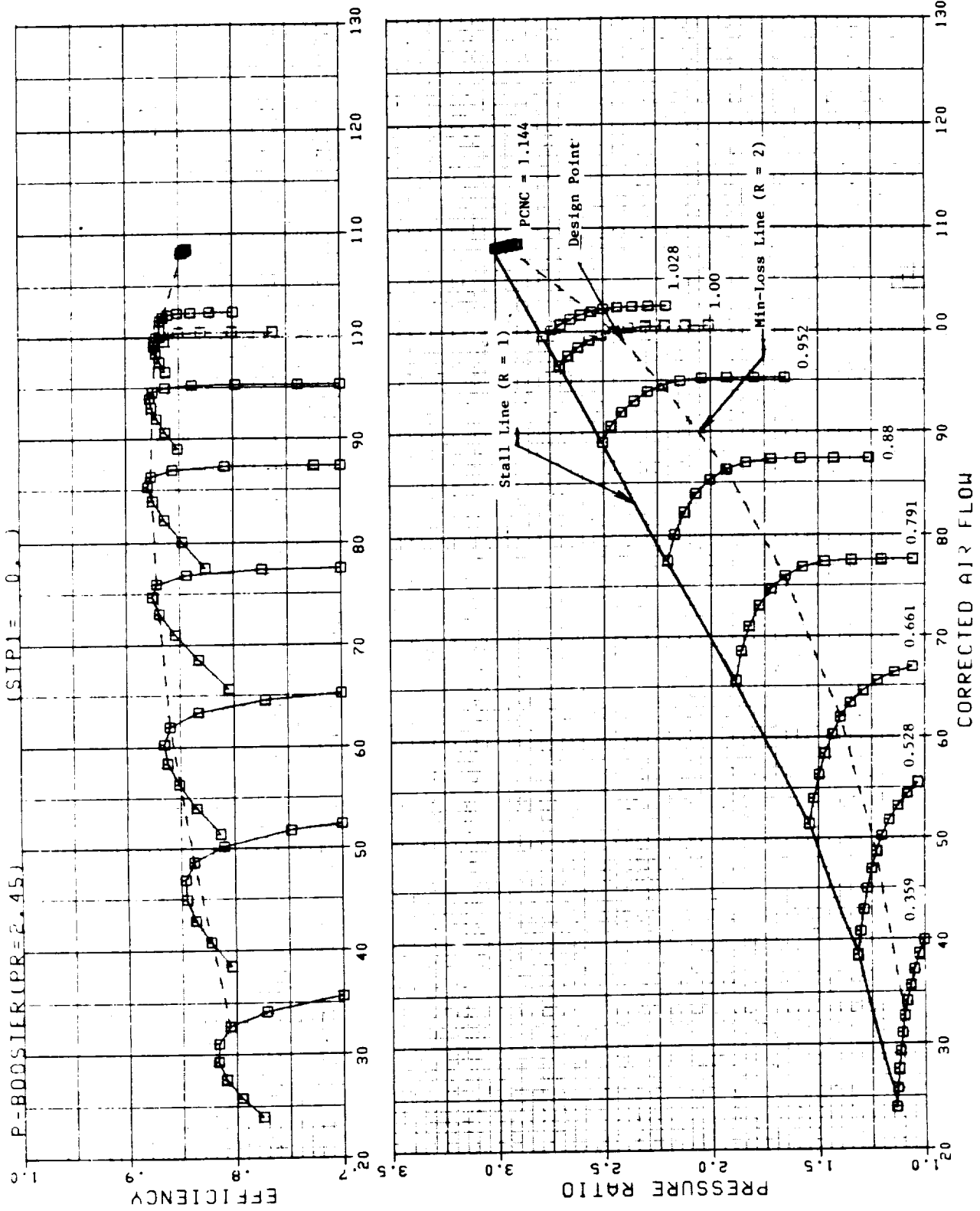


Figure 5. Parametric Booster Performance Map (PR = 2.45).

4.0 PROGRAM OUTPUTS

The basic output from the program consists of three tables. These tables show the variation in corrected flow, efficiency, and pressure ratio for each of the stator schedules, R-values, and corrected speeds specified in the input. The low T2 and high T2 stator schedules are written in the output file as pseudo-angle positions of zero and ninety degrees. The output tables for the second default case are shown on pages 19,20, & 21. The table structure is compatible with NASA cycle deck requirements given in Reference 2 (pages A23 and A24).

The output tables can be visualized as three dimensional, composed of a series of planes with each plane assigned a value of pseudo-angle position, ANGL. Then in each ANGL plane, the dependent variable (ordinate axis) is a function of corrected speed, SPED, and R value. The dependent variables are respectively corrected flow, total-to-total efficiency, and pressure ratio.

For example, in the output table on page 24 the 18 lines of the dependent variable correspond to the 9 values of corrected speed, two lines per speed. Within each speed there are 11 R values.

It should be noted that for pressure ratios less than unity the efficiency is negative (see discussion in section 7). These efficiency values are not incorrect, however, the efficiency behavior in this region makes curve fitting and interpolation of efficiency values extremely difficult. For this reason many engine manufacturers use some form of locus or temperature ratio parameter rather than efficiency for interpolation. The solution used here was to simply discard the information below unity pressure ratio and to display the solution for unity pressure ratio for all values of R at which the pressure ratio is less than unity. This means that identical values of pressure ratio (PR=1.0), flow and efficiency (EFF=0.0) will appear in the output table on any speed line where the value of R results in a pressure ratio less than unity.

5.0 PROGRAM DIAGNOSTICS

The CMGEN computer program contains several diagnostic error messages to aid the user in trouble shooting his input. A listing of the error messages and their meanings are given below.

1. ITERATION COUNTER EXCEEDED, GHS, PQW, PQWS

This fatal error occurs if no stall intersection can be found at the design speed. The program stops. The user should reduce the input value of the stall margin, STMRGN.

2. FLOW IS ZERO

This fatal error occurs for the same reason as the one above, however, in this case the flow has reached zero before the iteration counter has been exceeded. The input stall margin, STMRGN, should be reduced.

3. WARNING: NO STALL SOLUTION FOUND AT PCN=, F7.3

This warning error occurs if no stall intersection is found at a speed other than the design speed. Stall is assumed to occur at zero corrected flow. Program continues. The input stall margin should be reduced and/or the range of speeds restricted. If the value of speed displayed by the warning message is outside the range of interest the latter fix can be used.

4. QIRE CTR ERROR - - (CALLING LINE =, I5)

There is one iteration of this type in the program. This iteration is balanced using the Method of False Position. This method is contained in the subroutine QIREXX. A maximum of 25 passes is allowed for any single iteration to balance. If the iteration does not balance within the specified tolerance, the error message will appear with the statement number of the calling line in the I5 Format field.

This iteration was used to obtain the value of the corrected flow for unity pressure ratio. The value of I5 will be 624. The program will use the largest value of flow obtained in the 25 passes and continue. The user should inspect his output data at

unity pressure ratio to see if the flow speed relationship is smooth. The user can restrict the range of R values so that the pressure ratio is always greater than unity.

6.0 EXAMPLE CASES

Two example cases are given in order to illustrate the use of the program. The first case utilizes the default settings to generate the output for a twelve-to-one core compressor. The second case is that of a fixed geometry booster. In both cases the design point is at $R=2$ and $speed=1$.

A complete record of the two terminal sessions including a listing of the output tables is given on the following pages. The program inputs and outputs have been discussed in Section 3.0 and 4.0.

PARAMETRIC FAN, BOOSTER, AND COMPRESSOR GENERATOR

VARIABLE NAMES USED IN NAMELIST INPUT

NAME	DESCRIPTION
ITYPE	COMP TYPE: 1-FAN, 2-BOOSTER, 3-COMPRESSOR
PRDSGN	DESIGN POINT VALUE OF: PRESSURE RATIO
FLWDGN	CORRECTED FLOW
WQADGN	CORRECTED FLOW PER UNIT ANNULUS AREA
ETADGN	EFFICIENCY
UTRD	CORRECTED FIRST STAGE ROTOR TIP SPEED
STMRGN	CONSTANT SPEED STALL MARGIN
NR	NO OF R VALUES
AR	ARRAY OF R VALUES
NSPDS	NO OF CORRECTED SPEEDS
APCNC	ARRAY OF CORRECTED SPEEDS

```

NAMELIST INPUT
ITYPE= 3
PRDSGN= 12.000000, FLWDGN= 165.000000
WQADGN= 40.000000, ETADGN= 0.851000
UTRD = 1000.000000, STMRGN= 15.000000
NSPDS = 12,
APCNC (I)=
  1 0.100000, 0.200000, 0.300000, 0.400000,
  5 0.500000, 0.600000, 0.700000, 0.800000,
  9 0.900000, 1.000000, 1.100000, 1.200000,
 13 1.300000, 1.300000, 1.300000,
NR = 11,
AR (I)=
  1 1.000000, 1.200000, 1.400000, 1.600000,
  5 1.800000, 2.000000, 2.200000, 2.400000,
  9 2.600000, 2.800000, 3.000000, 3.200000,
 13 3.200000, 3.200000, 3.200000,
END NAMELIST

```

ENTER CHANGES TO NAMELIST INPUT

=SINPUTS

```

NAMELIST INPUT
ITYPE= 3
PRDSGN= 12.000000, FLWDGN= 165.000000
WQADGN= 40.000000, ETADGN= 0.851000
UTRD = 1000.000000, STMRGN= 15.000000
NSPDS = 12,
APCNC (I)=
  1 0.100000, 0.200000, 0.300000, 0.400000,
  5 0.500000, 0.600000, 0.700000, 0.800000,
  9 0.900000, 1.000000, 1.100000, 1.200000,
 13 1.300000, 1.300000, 1.300000,
NR = 11,
AR (I)=
  1 1.000000, 1.200000, 1.400000, 1.600000,
  5 1.800000, 2.000000, 2.200000, 2.400000,
  9 2.600000, 2.800000, 3.000000, 3.200000,

```

ORIGINAL PAGE IS
OF POOR QUALITY

13 3.200000, 3.200000, 3.200000.
END NAMELIST
MAP FILE ON TEMP FILE 22
YOU HAVE CREATED TEMP FILE 22
NASA OUTPUT ON FILE CODES 30,31,AND 32 &

ORIGINAL PAGE IS
OF POOR QUALITY

3001 P-COMPRESSOR FLOW VS. R. SPEED. AND ANGL								
ANGL	2	0.0	90.000					
SPED	12	0.100	0.200	0.300	0.400	0.500	0.600	0.700
SPED	12	0.800	0.900	1.000	1.100	1.200		
R	11	1.000	1.200	1.400	1.600	1.800	2.000	2.200
R	11	2.400	2.600	2.800	3.000			
FLOW	11	2.4243	2.9874	3.5304	4.0500	4.5433	5.0076	5.4409
FLOW	11	5.4605	5.4605	5.4605	5.4605			
FLOW	11	6.9268	7.5854	8.2244	8.8427	9.4389	10.0118	10.5604
FLOW	11	10.9181	10.9181	10.9181	10.9181			
FLOW	11	12.4354	13.1153	13.7702	14.3993	15.0017	15.5768	16.1241
FLOW	11	16.6431	17.1334	17.1476	17.1476			
FLOW	11	17.8595	18.6732	19.4455	20.1754	20.8623	21.5058	22.1053
FLOW	11	22.6609	23.1725	23.5855	23.5855			
FLOW	11	24.1855	25.2298	26.1979	27.0890	27.9027	28.6390	29.2984
FLOW	11	29.8818	30.3903	30.8255	30.9835			
FLOW	11	33.6833	34.6643	35.5577	36.3640	37.0838	37.7187	38.2697
FLOW	11	38.7389	39.1283	39.4404	39.6777			
FLOW	11	47.3011	48.1558	48.9154	49.5821	50.1577	50.6441	51.0438
FLOW	11	51.3595	51.5938	51.7498	51.8306			
FLOW	11	68.6262	69.5158	70.2900	70.9513	71.5025	71.9469	72.2876
FLOW	11	72.5280	72.6721	72.7235	72.7238			
FLOW	11	107.5632	108.9274	110.0945	111.0690	111.8568	112.4642	112.8965
FLOW	11	113.1608	113.2641	113.2660	113.2660			
FLOW	11	152.8882	153.4332	153.9158	154.3369	154.6978	154.9999	155.2434
FLOW	11	155.4298	155.5605	155.6367	155.6595			
FLOW	11	162.7337	162.8315	162.9242	163.0103	163.0921	163.1680	163.2384
FLOW	11	163.3034	163.3629	163.4173	163.4664			
FLOW	11	168.3818	168.3885	168.3941	168.4001	168.4058	168.4113	168.4163
FLOW	11	168.4215	168.4262	168.4304	168.4345			
SPED	12	0.100	0.200	0.300	0.400	0.500	0.600	0.700
SPED	12	0.800	0.900	1.000	1.100	1.200		
R	11	1.000	1.200	1.400	1.600	1.800	2.000	2.200
R	11	2.400	2.600	2.800	3.000			
FLOW	11	5.9010	6.4179	6.9201	7.4065	7.8761	8.3284	8.7624
FLOW	11	9.0820	9.0820	9.0820	9.0820			
FLOW	11	15.3025	15.7660	16.2153	16.6501	17.0703	17.4756	17.8659
FLOW	11	18.2410	18.6010	18.9455	19.2401			
FLOW	11	25.0730	25.2443	25.4121	25.5766	25.7378	25.8956	26.0500
FLOW	11	26.2011	26.3489	26.4933	26.6343			
FLOW	11	35.2710	35.6607	36.0294	36.3775	36.7050	37.0123	37.2992
FLOW	11	37.5658	37.8129	38.0403	38.2483			
FLOW	11	46.5366	46.9060	47.2493	47.5667	47.8588	48.1257	48.3680
FLOW	11	48.5856	48.7794	48.9494	49.0964			
FLOW	11	59.6975	60.0498	60.3728	60.6669	60.9329	61.1710	61.3811
FLOW	11	61.5645	61.7212	61.8518	61.9570			
FLOW	11	76.3187	76.7204	77.0834	77.4080	77.6957	77.9466	78.1612
FLOW	11	78.3404	78.4850	78.5957	78.6731			
FLOW	11	97.4995	98.0523	98.5455	98.9795	99.3559	99.6760	99.9403
FLOW	11	100.1504	100.3072	100.4128	100.4677			
FLOW	11	125.6839	126.5036	127.2202	127.8359	128.3531	128.7742	129.1008
FLOW	11	129.3362	129.4829	129.5431	129.5451			
FLOW	11	152.9693	153.4906	153.9540	154.3589	154.7070	154.9999	155.2371
FLOW	11	155.4207	155.5515	155.6309	155.6596			
FLOW	11	162.7337	162.8315	162.9242	163.0103	163.0921	163.1680	163.2384
FLOW	11	163.3034	163.3631	163.4173	163.4664			
FLOW	11	168.3817	168.3885	168.3941	168.4000	168.4058	168.4113	168.4163
FLOW	11	168.4215	168.4262	168.4304	168.4345			
EOT								

ORIGINAL PAGE IS
OF POOR QUALITY

3002		P-COMPRESSOR EFF VS.		R. SPEED. AND ANGL				
ANGL	2	0.0	90.000					
SPED	12	0.100	0.200	0.300	0.400	0.500	0.600	0.700
SPED	12	0.800	0.900	1.000	1.100	1.200		
R	11	1.000	1.200	1.400	1.600	1.800	2.000	2.200
R	11	2.400	2.600	2.800	3.000			
EFF	11	0.8597	0.8364	0.8039	0.7992	0.7682	0.6713	0.0886
EFF	11	0.0	0.0	0.0	0.0			
EFF	11	0.8086	0.8037	0.7972	0.7797	0.7435	0.6713	0.4499
EFF	11	0.0	0.0	0.0	0.0			
EFF	11	0.7976	0.7897	0.7769	0.7573	0.7280	0.6840	0.5976
EFF	11	0.4126	0.0256	0.0	0.0			
EFF	11	0.7942	0.7857	0.7734	0.7559	0.7315	0.6974	0.6371
EFF	11	0.5221	0.3161	0.0	0.0			
EFF	11	0.7934	0.7864	0.7761	0.7615	0.7413	0.7136	0.6647
EFF	11	0.5729	0.4162	0.1547	0.0			
EFF	11	0.7900	0.7842	0.7763	0.7657	0.7519	0.7342	0.7051
EFF	11	0.6544	0.5759	0.4606	0.2952			
EFF	11	0.7992	0.7953	0.7900	0.7831	0.7743	0.7635	0.7460
EFF	11	0.7163	0.6721	0.6107	0.5286			
EFF	11	0.8286	0.8276	0.8255	0.8222	0.8177	0.8116	0.8000
EFF	11	0.7789	0.7463	0.7012	0.6418			
EFF	11	0.8528	0.8590	0.8632	0.8654	0.8652	0.8626	0.8489
EFF	11	0.8145	0.7575	0.6756	0.5664			
EFF	11	0.8519	0.8532	0.8538	0.8536	0.8527	0.8510	0.8459
EFF	11	0.8347	0.8171	0.7929	0.7617			
EFF	11	0.8088	0.8084	0.8077	0.8067	0.8054	0.8037	0.8008
EFF	11	0.7955	0.7878	0.7776	0.7649			
EFF	11	0.7587	0.7578	0.7569	0.7558	0.7547	0.7534	0.7518
EFF	11	0.7494	0.7462	0.7423	0.7377			
SPED	12	0.100	0.200	0.300	0.400	0.500	0.600	0.700
SPED	12	0.800	0.900	1.000	1.100	1.200		
R	11	1.000	1.200	1.400	1.600	1.800	2.000	2.200
R	11	2.400	2.600	2.800	3.000			
EFF	11	0.8038	0.8030	0.7954	0.7771	0.7410	0.6713	0.4691
EFF	11	0.0	0.0	0.0	0.0			
EFF	11	0.7807	0.7703	0.7569	0.7396	0.7172	0.6884	0.6437
EFF	11	0.5692	0.4509	0.2651	0.0			
EFF	11	0.7411	0.7353	0.7291	0.7225	0.7153	0.7075	0.6986
EFF	11	0.6879	0.6753	0.6605	0.6434			
EFF	11	0.7706	0.7648	0.7583	0.7508	0.7423	0.7328	0.7204
EFF	11	0.7032	0.6805	0.6518	0.6159			
EFF	11	0.7845	0.7804	0.7758	0.7705	0.7646	0.7580	0.7494
EFF	11	0.7372	0.7212	0.7010	0.6761			
EFF	11	0.8053	0.8026	0.7995	0.7960	0.7920	0.7875	0.7814
EFF	11	0.7726	0.7607	0.7457	0.7272			
EFF	11	0.8350	0.8337	0.8320	0.8298	0.8272	0.8241	0.8191
EFF	11	0.8107	0.7989	0.7832	0.7636			
EFF	11	0.8576	0.8582	0.8581	0.8573	0.8558	0.8535	0.8480
EFF	11	0.8367	0.8193	0.7953	0.7645			
EFF	11	0.8611	0.8639	0.8656	0.8661	0.8655	0.8635	0.8560
EFF	11	0.8383	0.8099	0.7699	0.7178			
EFF	11	0.8522	0.8533	0.8538	0.8536	0.8527	0.8510	0.8461
EFF	11	0.8355	0.8189	0.7960	0.7665			
EFF	11	0.8088	0.8084	0.8077	0.8067	0.8054	0.8037	0.8008
EFF	11	0.7955	0.7878	0.7776	0.7649			
EFF	11	0.7587	0.7578	0.7569	0.7558	0.7547	0.7534	0.7518
EFF	11	0.7494	0.7462	0.7423	0.7377			
EOT								

ORIGINAL PAGE 11
OF POOR QUALITY

3003	P-COMPRESSOR	PR VS.	R.	SPEED.	AND	ANGL		
ANGL 2	0 0	90.000						
SPED 12	0.100	0.200	0.300	0.400	0.500	0.600	0.700	
SPED 12	0.800	0.900	1.000	1.100	1.200			
R 11	1.000	1.200	1.400	1.600	1.800	2.000	2.200	
R 11	2.400	2.600	2.800	3.000				
PR 11	1.0578	1.0480	1.0384	1.0305	1.0220	1.0128	1.0009	
PR 11	1.0000	1.0000	1.0000	1.0000				
PR 11	1.1650	1.1431	1.1215	1.0991	1.0759	1.0519	1.0238	
PR 11	1.0000	1.0000	1.0000	1.0000				
PR 11	1.2962	1.2637	1.2309	1.1977	1.1641	1.1303	1.0933	
PR 11	1.0505	1.0023	1.0000	1.0000				
PR 11	1.5356	1.4807	1.4259	1.3711	1.3165	1.2622	1.2041	
PR 11	1.1387	1.0672	1.0000	1.0000				
PR 11	1.9816	1.8846	1.7883	1.6930	1.5988	1.5061	1.4075	
PR 11	1.2972	1.1780	1.0527	1.0000				
PR 11	2.6731	2.5349	2.3984	2.2637	2.1312	2.0012	1.8640	
PR 11	1.7121	1.5493	1.3794	1.2064				
PR 11	3.7448	3.5620	3.3810	3.2023	3.0260	2.8527	2.6697	
PR 11	2.4670	2.2491	2.0207	1.7870				
PR 11	5.4863	5.2552	5.0232	4.7910	4.5592	4.3284	4.0769	
PR 11	3.7868	3.4657	3.1218	2.7637				
PR 11	9.1205	8.8537	8.5563	8.2309	7.8801	7.5072	7.0115	
PR 11	6.3163	5.4701	4.5316	3.5655				
PR 11	13.6119	13.3192	13.0106	12.6872	12.3500	12.0000	11.5760	
PR 11	11.0268	10.3644	9.6063	8.7719				
PR 11	14.6504	14.3973	14.1379	13.8726	13.6018	13.3257	13.0157	
PR 11	12.6453	12.2183	11.7393	11.2136				
PR 11	15.2538	15.0727	14.8897	14.7050	14.5187	14.3307	14.1305	
PR 11	13.9080	13.6640	13.3993	13.1150				
SPED 12	0.100	0.200	0.300	0.400	0.500	0.600	0.700	
SPED 12	0.800	0.900	1.000	1.100	1.200			
R 11	1.000	1.200	1.400	1.600	1.800	2.000	2.200	
R 11	2.400	2.600	2.800	3.000				
PR 11	1.1080	1.0947	1.0807	1.0663	1.0513	1.0357	1.0175	
PR 11	1.0000	1.0000	1.0000	1.0000				
PR 11	1.3006	1.2740	1.2473	1.2205	1.1936	1.1667	1.1381	
PR 11	1.1066	1.0724	1.0355	1.0000				
PR 11	1.4875	1.4698	1.4522	1.4346	1.4171	1.3997	1.3819	
PR 11	1.3636	1.3447	1.3253	1.3053				
PR 11	2.2703	2.2060	2.1421	2.0788	2.0160	1.9539	1.8900	
PR 11	1.8222	1.7508	1.6764	1.5993				
PR 11	3.1211	3.0303	2.9402	2.8509	2.7623	2.6746	2.5843	
PR 11	2.4880	2.3864	2.2802	2.1701				
PR 11	4.1121	4.0014	3.8911	3.7814	3.6725	3.5642	3.4519	
PR 11	3.3312	3.2028	3.0677	2.9267				
PR 11	5.4241	5.2863	5.1479	5.0091	4.8702	4.7311	4.5828	
PR 11	4.4172	4.2359	4.0405	3.8329				
PR 11	7.3013	7.1247	6.9431	6.7568	6.5663	6.3720	6.1498	
PR 11	5.8782	5.5626	5.2088	4.8237				
PR 11	10.4205	10.1680	9.8971	9.6091	9.3052	8.9870	8.5879	
PR 11	8.0516	7.3984	6.6530	5.8434				
PR 11	13.5715	13.2850	12.9837	12.6685	12.3402	12.0000	11.5904	
PR 11	11.0611	10.4246	9.6964	8.8939				
PR 11	14.6504	14.3973	14.1379	13.8726	13.6018	13.3257	13.0157	
PR 11	12.6453	12.2183	11.7393	11.2136				
PR 11	15.2538	15.0727	14.8897	14.7050	14.5187	14.3307	14.1305	
PR 11	13.9080	13.6640	13.3993	13.1150				
EOT								

ORIGINAL PAGE IS
OF POOR QUALITY

PARAMETRIC FAN, BOOSTER, AND COMPRESSOR GENERATOR

VARIABLE NAMES USED IN NAMELIST INPUT

NAME	DESCRIPTION
ITYPE	COMP TYPE: 1=FAN, 2=BOOSTER, 3=COMPRESSOR
PRDSGN	DESIGN POINT VALUE OF:
FLVDGN	PRESSURE RATIO
WQADGN	CORRECTED FLOW
ETADGN	CORRECTED FLOW PER UNIT ANNULUS AREA
UTRD	EFFICIENCY
STMRGN	CORRECTED FIRST STAGE ROTOR TIP SPEED
	CONSTANT SPEED STALL MARGIN
NR	NO OF R VALUES
AR	ARRAY OF R VALUES
NSPDS	NO OF CORRECTED SPEEDS
APCNC	ARRAY OF CORRECTED SPEEDS

```

NAMELIST INPUT
ITYPE= 3
PRDSGN= 12.000000, FLVDGN= 155.000000
WQADGN= 40.000000, ETADGN= 0.851000
UTRD = 100.000000, STMRGN= 15.000000
NSPDS = 12,
APCNC (I)=
  1 0.100000, 0.200000, 0.300000, 0.400000,
  5 0.500000, 0.600000, 0.700000, 0.800000,
  9 0.900000, 1.000000, 1.100000, 1.200000,
 13 1.300000, 1.300000, 1.300000,
NR = 11,
AR (I)=
  1 1.000000, 1.200000, 1.400000, 1.600000,
  5 1.800000, 2.000000, 2.200000, 2.400000,
  9 2.600000, 2.800000, 3.000000, 3.200000,
 13 3.200000, 3.200000, 3.200000,

```

```

END NAMELIST
ENTER CHANGES TO NAMELIST INPUT
=SINPUT ITYPE=2, PRDSGN=2.45, FLVDGN=200.5, WQADGN=33.7,
=ETADGN=.844, UTRD=869.7, STMRGN=14.34,
=NSPDS/APCNC=.359,.528,.661,.791,.88,.952,1.0,1.028,1.144$

```

```

NAMELIST INPUT
ITYPE= 2
PRDSGN= 2.450000, FLVDGN= 200.500000
WQADGN= 33.700000, ETADGN= 0.844000
UTRD = 869.699997, STMRGN= 14.340000
NSPDS = 9,
APCNC (I)=
  1 0.359000, 0.528000, 0.661000, 0.791000,
  5 0.800000, 0.952000, 1.000000, 1.028000,
  9 1.144000, 1.000000, 1.100000, 1.200000,
 13 1.300000, 1.300000, 1.300000,
NR = 11,
AR (I)=
  1 1.000000, 1.200000, 1.400000, 1.600000,

```

5	1.800000,	2.000000,	2.200000,	2.400000,
9	2.600000,	2.800000,	3.000000,	3.200000,
13	3.200000,	3.200000,	3.200000,	

END NAMELIST
MAP FILE ON TEMP FILE 22
YOU HAVE CREATED TEMP FILE 22
NASA OUTPUT ON FILE CODES 30,31,AND 32 &

ORIGINAL PAGE IS
OF POOR QUALITY

2001		P-BOOSTER FLOW VS. R. SPEED, AND ANGL						
ANGL	1	0.0						
SPED	9	0.359	0.528	0.661	0.791	0.880	0.952	1.000
SPED	9	1.028	1.144					
R	11	1.000	1.200	1.400	1.600	1.800	2.000	2.200
R	11	2.400	2.600	2.800	3.000			
FLOW	11	69.3296	74.5637	79.6694	84.6391	89.4656	94.1431	98.6653
FLOW	11	103.0265	107.2229	111.2497	114.6824			
FLOW	11	111.3183	117.7914	123.9229	129.7021	135.1212	140.1741	144.8552
FLOW	11	149.1636	153.0977	156.6591	159.8508			
FLOW	11	148.4324	155.7878	162.4920	168.5404	173.9307	178.6670	182.7580
FLOW	11	186.2159	189.0569	191.3010	192.9713			
FLOW	11	189.8559	198.0533	205.0578	210.8891	215.5753	219.1571	221.6829
FLOW	11	223.2093	223.7980	223.8097	223.8097			
FLOW	11	224.2483	231.3824	237.3943	242.3121	246.1686	249.0090	250.8790
FLOW	11	251.8331	251.9902	251.9902	251.9902			
FLOW	11	257.2646	261.7246	265.4973	268.6003	271.0571	272.8899	274.1228
FLOW	11	274.7837	274.9211	274.9211	274.9211			
FLOW	11	279.0522	281.6934	283.9485	285.8279	287.3408	288.4990	289.3119
FLOW	11	289.7942	289.9558	289.9561	289.9561			
FLOW	11	287.3101	289.1123	290.6746	292.0032	293.1016	293.9771	294.6343
FLOW	11	295.0789	295.3181	295.3667	295.3667			
FLOW	11	311.8733	312.0000	312.1238	312.2412	312.3530	312.4617	312.5637
FLOW	11	312.6604	312.7522	312.8386	312.9202			
EOT								

ORIGINAL COPY
OF PUNCH TAPE

2002		P-BOOSTER EFF VS. R. SPEED. AND ANGL						
ANGL	1	0.0						
SPED	9	0.359	0.528	0.661	0.791	0.880	0.952	1.000
SPED	9	1.028	1.144					
R	11	1.000	1.200	1.400	1.600	1.800	2.000	2.200
R	11	2.400	2.600	2.800	3.000			
EFF	11	0.7584	0.7770	0.7900	0.7963	0.7940	0.7811	0.7430
EFF	11	0.6631	0.5232	0.3001	0.0			
EFF	11	0.7862	0.8037	0.8162	0.8228	0.8206	0.8122	0.7819
EFF	11	0.7153	0.6009	0.4217	0.1514			
EFF	11	0.7948	0.8151	0.8302	0.8392	0.8408	0.8331	0.8043
EFF	11	0.7381	0.6233	0.4430	0.1721			
EFF	11	0.7866	0.8126	0.8328	0.8460	0.8506	0.8447	0.8144
EFF	11	0.7407	0.6108	0.4056	0.0969			
EFF	11	0.8067	0.8266	0.8417	0.8512	0.8542	0.8496	0.8279
EFF	11	0.7774	0.6917	0.5626	0.3792			
EFF	11	0.8303	0.8403	0.8474	0.8513	0.8515	0.8477	0.8254
EFF	11	0.8095	0.7681	0.7091	0.6299			
EFF	11	0.8397	0.8442	0.8470	0.8481	0.8471	0.8440	0.8366
EFF	11	0.8226	0.8012	0.7719	0.7340			
EFF	11	0.8399	0.8419	0.8429	0.8426	0.8412	0.8386	0.8234
EFF	11	0.8243	0.8112	0.7938	0.7716			
EFF	11	0.8223	0.8219	0.8215	0.8210	0.8205	0.8200	0.8195
EFF	11	0.8188	0.8182	0.8174	0.8166			
EOT								

ORIGINAL PAGE IS
OF POOR QUALITY

2003		P-BOOSTER PR VS. R. SPEED. AND ANGL						
ANGL	1	0.0						
SPED	9	0.359	0.528	0.661	0.791	0.980	0.952	1.000
SPED	9	1.028	1.144					
R	11	1.000	1.200	1.400	1.600	1.800	2.000	2.200
R	11	2.400	2.600	2.800	3.000			
PR	11	1.1370	1.1316	1.1248	1.1168	1.1074	1.0968	1.0837
PR	11	1.0670	1.0469	1.0235	1.0000			
PR	11	1.3169	1.3042	1.2888	1.2708	1.2503	1.2273	1.1995
PR	11	1.1647	1.1234	1.0762	1.0237			
PR	11	1.5447	1.5245	1.4992	1.4689	1.4339	1.3946	1.3465
PR	11	1.2860	1.2145	1.1334	1.0446			
PR	11	1.8882	1.8616	1.8242	1.7765	1.7191	1.6527	1.5691
PR	11	1.4615	1.3340	1.1913	1.0386			
PR	11	2.2086	2.1738	2.1277	2.0708	2.0038	1.9274	1.8328
PR	11	1.7129	1.5718	1.4141	1.2452			
PR	11	2.5106	2.4677	2.4172	2.3595	2.2950	2.2241	2.1405
PR	11	2.0386	1.9207	1.7890	1.6462			
PR	11	2.7096	2.6663	2.6185	2.5664	2.5101	2.4500	2.3818
PR	11	2.3021	2.2115	2.1113	2.0026			
PR	11	2.7840	2.7435	2.7003	2.6544	2.6060	2.5552	2.4994
PR	11	2.4360	2.3655	2.2885	2.2055			
PR	11	3.0007	2.9912	2.9817	2.9722	2.9625	2.9529	2.9431
PR	11	2.9331	2.9229	2.9126	2.9021			
EOT								

7.0 ANALYTICAL BACKGROUND

7.1 COMPRESSOR MAP FITTING SYSTEM

A continuing effort has been conducted by The Aircraft Engine Business Group to obtain more efficient cycle decks. The effort included a search for ways to reduce the size of the computer memory required to represent component maps without compromising the accuracy of the component representations. Meeting both goals was a challenge, for they seemed to call for contrary design approaches. For this reason, new types of component map representations were explored. It was found that maps based on similarity parameters derived from the basic physics of the components produced component maps of equivalent accuracy while requiring less computer memory. Moreover, the use of map "fits" based upon variables obtained from the physics of the component resulted in generally smoother maps and a more meaningful extrapolation to regions not covered by the data. This approach is especially well suited to parametric component representations, for parametric maps can easily occupy a great deal of computer memory. Parametric compressor maps, for example, require computer memory for storage of the base map and the variations from the base map resulting from changes in the pressure ratio. The larger the range of pressure ratio, the more memory required. Add a second parameter, such as fan inlet guide vane angle, and memory requirements multiply rapidly.

Most of the parametric fan/compressor generating programs currently employed by AEBG are based on the map fitting procedure to fit fan and compressor performance maps prior to their inclusion in a cycle deck. For this reason, a description of the map fitting procedure currently being used is necessary in order to gain an understanding of the parameteric fan/compressor generating programs.

In the following sections a brief description of the map fitting procedure will be given. The section also contains sufficient component performance background information for the reader to gain an understanding of the similarity parameters employed in the map representation. The relationships required to define a map in the map fitting system are the specification of flow coefficient, work coefficient, and loss along the minimum loss locus which forms the "backbone" of the map; and the loss and flow variations along the speed lines.

7.1.1 DESCRIPTION OF CURRENT COMPRESSOR MAP FITTING PROCEDURE

A typical compressor performance map is shown in Figure 1. Corrected air flow is the abscissa, and total-to-total pressure ratio is the ordinate. Lines of constant corrected speed and constant efficiency contours are plotted. In addition to the map performance parameters, design point values of first stage rotor tip speed (ω_{Tip} , ft/sec) and inlet specific flow (W_{corr}/A , lbm/sec/ft²) are required in order to fit the map.

Some additional parameters used in the fitting procedure are defined from the entropy-enthalpy diagram of a compressor stage. These parameters are shown in Figure 6.

7.1.2 GENERAL BACKGROUND

The compressor stage characteristic serves as the basis for the map fitting procedure. An analytical expression for the stage characteristic of a constant-pitch, axial-flow compressor can be obtained by using the steady flow energy and angular momentum equations, together with a number of relationships from the pitch line vector diagram. In deriving this equation, it is assumed that the pitch line flow angle at rotor and stator exit are in-variant and that the axial velocity ratio across the rotor is constant.

The stage characteristic for a single-stage compressor with the above assumptions can be written in the form -

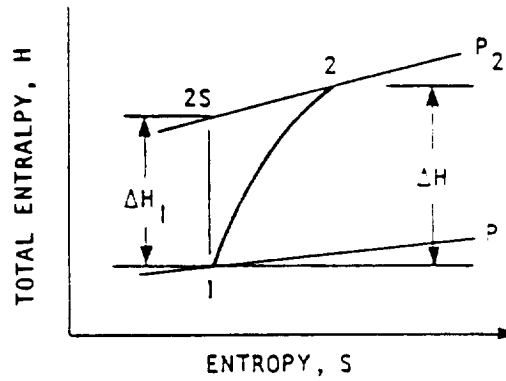
$$\psi = 2 - 2\phi (\tan \alpha_1 + C_{z2}/C_{z1} \tan \beta_2) \quad (1)$$

The equation is a straight line (ψ vs. ϕ Plot) passing through the point ($\psi = 2, \phi = 0$).

A typical low speed compressor stage characteristic is shown in Figure 7. In practice, it is found that in the neighborhood of the peak efficiency changes in the absolute air inlet angle and the relative air-outlet angle are small. They can, however, change considerably at extreme operating conditions. The key point is that in the high efficiency region change in the stage characteristic is nearly linear.

A loss parameter as defined by the difference between the values of the work coefficient and the pressure coefficient is introduced as illustrated in figure 8. Figure 8-A shows an idealized stage characteristic. In Figure 8-B the variation in efficiency with flow coefficient has been shown. Note that the efficiency is zero at unity pressure ratio and has a singularity at the $\psi = 0$ point. This behavior makes the efficiency an inconvenient measure of performance in the neighborhood of zero work. If this behavior is contrasted with that of the loss as shown in Figure 8-C, the reasoning for the use of loss becomes evident. The loss is always positive, finite, and exhibits a minimum value. The map fitting procedure is built around the stage characteristic and the attendant concept of loss. The min-loss point is defined as the "backbone" point on the characteristic.

ORIGINAL PAGE IS
OF POOR QUALITY



LET: C_{z_1} = AXIAL VELOCITY COMPONENT AT ROTOR INLET

v = WHEEL SPEED

- DEFINE:
1. WORK COEFFICIENT, $\psi = \Delta H / (v^2 / 2g_o J)$
 2. PRESSURE COEFFICIENT, $\psi_1 = \Delta H_1 / (v^2 / 2g_o J)$
 3. FLOW COEFFICIENT, $\phi = C_{z_1} / v$
 4. EFFICIENCY, $EFF = \psi_1 / \psi$
 5. LOSS, $XLS = (\Delta H - \Delta H_1) / (v^2 / 2g_o J) = \psi - \psi_1$

Since $\eta = \frac{\psi_1}{\psi}$ and $Loss = \psi - \psi_1$

Then $Loss = \psi(1 - \eta)$ or $\eta = 1 - \frac{Loss}{\psi}$

Figure 6. Dimensionless Compressor Performance Parameters.

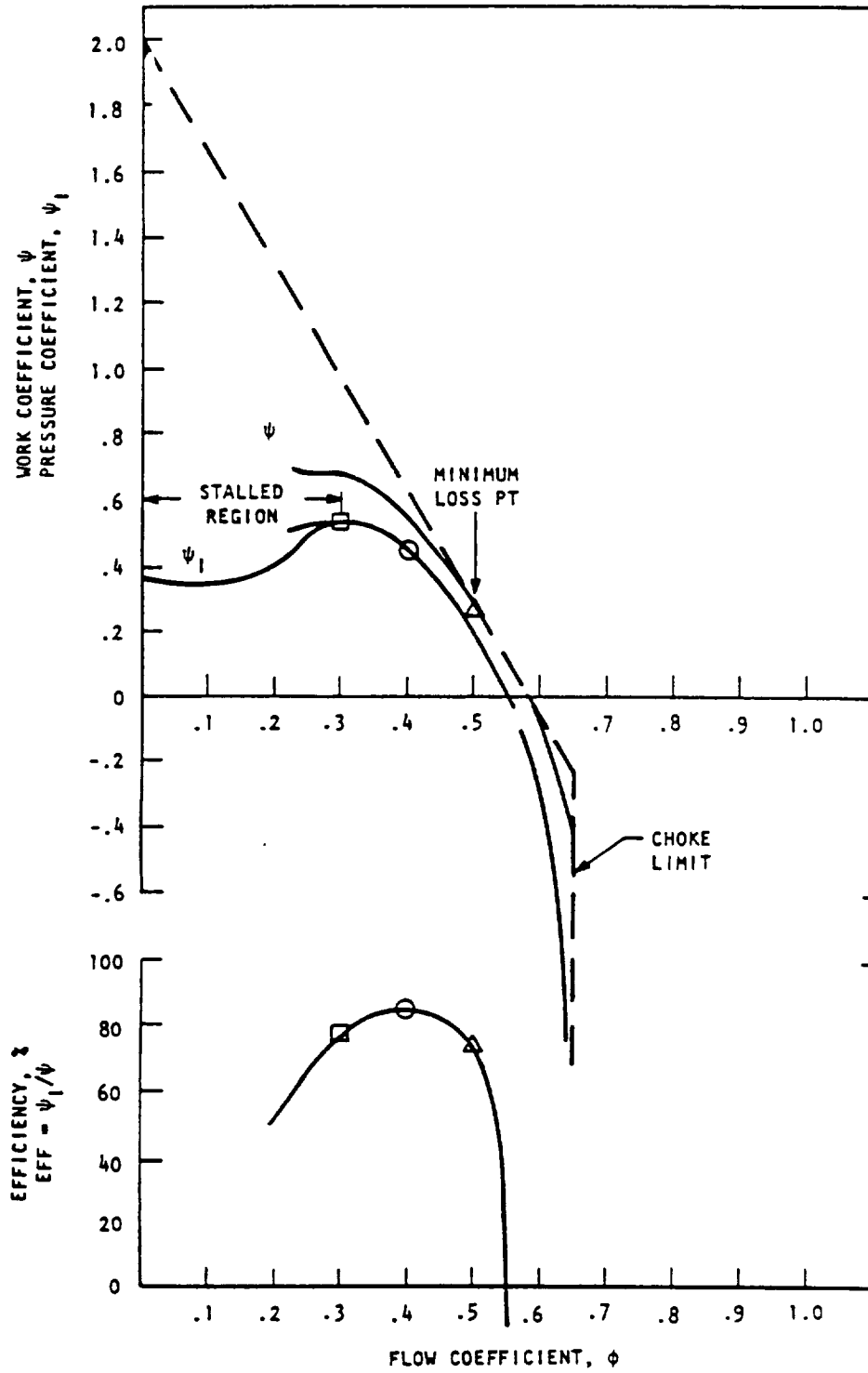


Figure 7. Compressor Stage Characteristic.

7.1.3 COMPRESSOR EFFICIENCY REPRESENTATION

The efficiency representation of the compressor is illustrated by the three sketches shown in Figure 9. For each map speed a plot of loss $(\psi - \psi_I)$ against work coefficient is constructed. Figure 9-A illustrates this type of plot. The values of work coefficient at min-loss (ψ_{ML}) and loss at min-loss $(\psi - \psi_I)_{ML}$ are picked off the curves for each value of speed. The locus of the min-loss points form the "backbone" of the map. The variation of ψ_{ML} and $(\psi - \psi_I)_{ML}$ are then plotted against speed as illustrated in Figure 9-B. The "off-backbone" loss is represented by a plot of the difference between the loss and the min-loss value at a given speed against the difference between the work coefficient and the min-loss work coefficient squared.

The sign of the work coefficient difference is used to plot the two branches of the bi-variate loss representation. When plotted in this fashion the loss correlation is nearly linear over a relatively wide range of work coefficient. However, breaks can occur in the neighborhood of positive stall and/or choking.

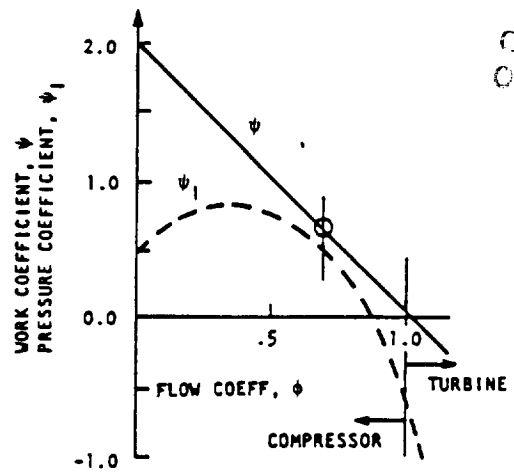
These three curves, two univariate and one bi-variate are sufficient to define the compressor efficiency. Since the three curves are fairly linear, a table look up is employed to obtain efficiency values in a cycle deck.

7.1.4 COMPRESSOR FLOW REPRESENTATION

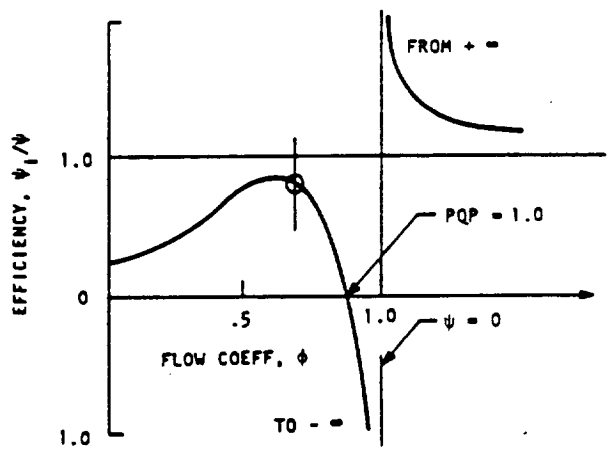
The flow representation begins by calculating the values of the flow coefficient at min-loss. Since the min-loss points on the map are known from the loss calculation, the flow at each min-loss point is known. The value of the inlet flow coefficient is then obtained from the flow-function Mach number relationship, i.e.,

$$(1) \quad \frac{W_{corr}}{Ann1} \Big|_{ML} = \frac{W_{corr}}{Ann1} \Big|_{Design} \frac{(W_{corr})_{ML}}{(W_{corr})_{Design}}$$

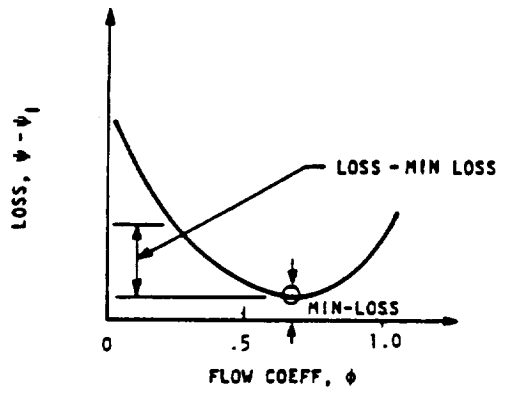
$$(2) \quad \frac{W_{corr}/Ann1}{\rho_{Tstd} A_{Tstd} \cos \alpha_1} = \frac{C_{z1}}{A_{T1}} \frac{1}{\cos \alpha_1} \left[1 - \frac{r-1}{z} \left(\frac{C_{z1}}{A_{T1}} \right)^2 \right]^{\frac{1}{r-1}} \frac{1}{\cos^2 \alpha_1} \quad \cos \alpha_1 = \frac{0}{A_{T1}} = \sqrt{r R g_0 T_1}$$



A STAGE CHARACTERISTIC

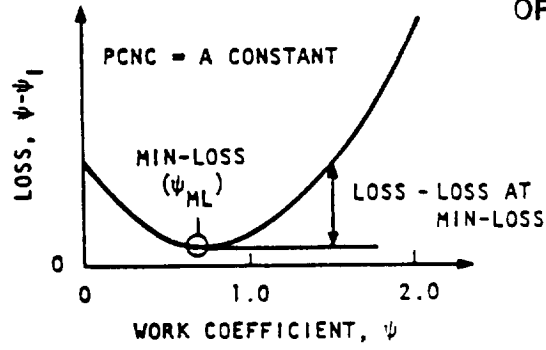


B EFFICIENCY CHARACTERISTIC

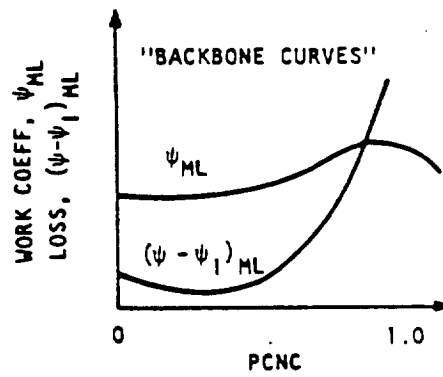


C LOSS CHARACTERISTIC

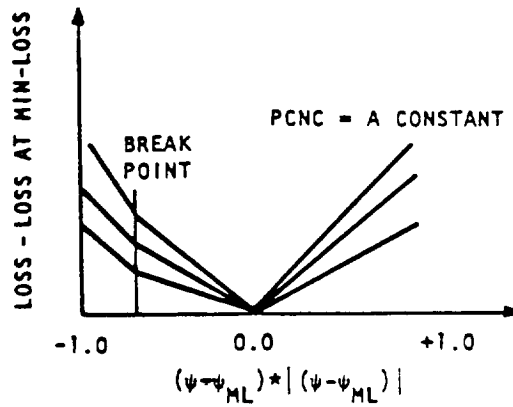
Figure 8. Compressor Loss Representation.



A. VARIATION OF LOSS WITH WORK COEFF.

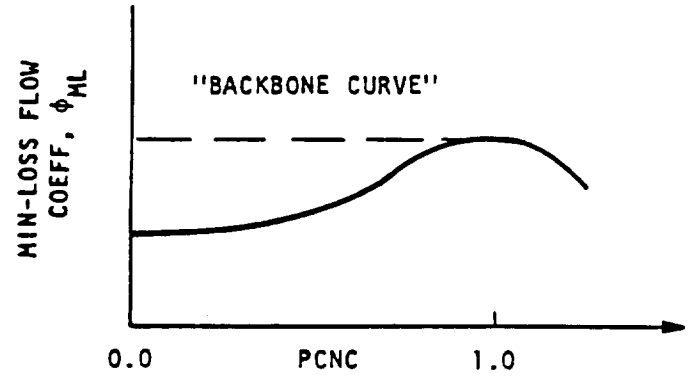


B. VARIATION OF MIN-LOSS
WORK COEFF. AND LOSS

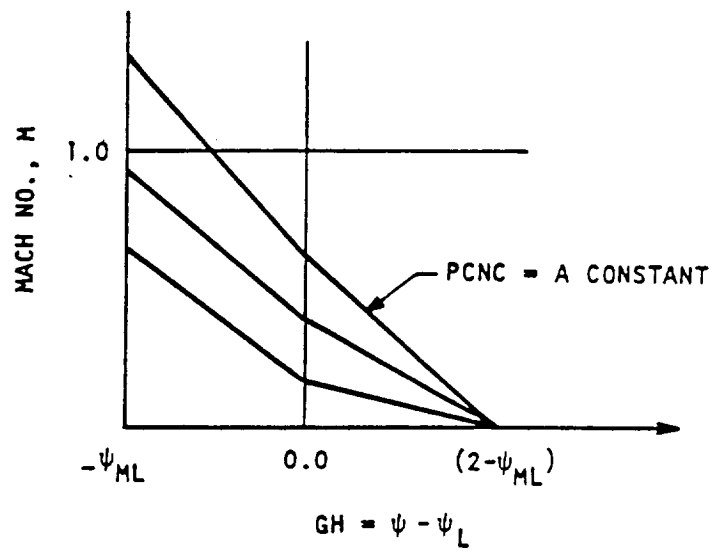


C. LOSS FUNCTION VARIATION

Figure 9. Stage Efficiency and Loss Characteristics.



A. VARIATION OF MIN-LOSS FLOW COEFFICIENT



B. MACH NUMBER VARIATION

Figure 10. Compressor Flow Representation.

$$(3) \quad v/A_{T1} = \text{PCNC} \cdot (v/AT_{\text{std}}) \text{ Design}$$

$$(4) \quad \phi_{ML} = \left(C_{z1}/A_{T1} \right) / \left(v/A_{T1} \right) = C_{z1} / v$$

A curve of min-loss flow coefficient as a function of speed as shown in Figure 10-A is then constructed. This univariate curve defines the flow along the "backbone" of the map.

The "off-backbone" flow is then obtained in the following manner. Consider the speed line sketch of Figure 1.

If we assume a pseudo Mach number somewhere in the machine of one at the maximum flow point, then a pseudo critical area can be calculated. If this pseudo area is assumed to remain constant along a speed line, a pseudo-Mach number can be defined at each point on the speed line as follows:

$$W_{\text{corr}} \quad W_{\text{corr}} \quad \text{max} = \left[M / \left(1 + \left(\frac{r+1}{2} \right) M^2 \right)^{\frac{r+1}{2(r-1)}} \right] \left(\frac{r+1}{2} \right)^{\frac{r+1}{2(r-1)}}$$

The Mach number is then plotted at each speed against $(\psi - \psi_{ML})$ as illustrated by Figure 10-B.

These two curves, one univariate and one bi-variate are sufficient to define the flow. As with the efficiency representation, these curves are fairly linear and a table look up is employed in the cycle deck evaluation.

7.1.5 COMPRESSOR BASE CURVES

These five curves, three univariate and two bi-variate are sufficient to define the performance map. These curves are part of the output from the CMGEN program and are written on File 22. They constitute an alternate map representation.

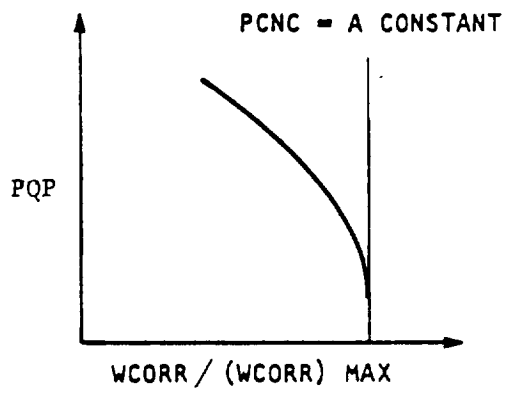


Figure 11. Speed Line Sketch.

7.2 DISCUSSION OF THE DERIVATION OF THE PARAMETRIC CURVE SETS

The activities of Preliminary Design organizations require the capability to rapidly generate a wide variety of fan and compressor maps for use in cycle analysis. The semi-empirical method adopted for the systematic generation of required maps is the subject of this section.

The approach adapted was to utilize, as directly as possible, the parameters that AEBG currently uses to fit performance caps. These required inputs to create a map are the specification of flow coefficient, work coefficient and loss along the minimum loss "BACKBONE" and the loss variation and flow variation along the speed lines.

Speed-flow relations have been of interest and the subject of much study over the years. Use of these relations and correlations from various compressor tests results in the flow coefficient-speed shown in Figure 12 with pressure ratio as the independent parameter. The speed-flow implied by Figure 12 for a design specific flow of 40 lbm/sec/ft^2 is shown in Figure 2. At a given flow coefficient ratio the percent flow depends upon the level of design Mach number and in this manner the speed-flow relation is dependent upon the design level of inlet specific flow, as it should be. This is illustrated in Figure 13, for a pressure ratio 12 design.

Work coefficient-speed relations are not convenient. Work coefficient-flow coefficient relations are more commonly used and in the early work on the method this type relation was employed. The work coefficient-speed relation was derived from the work coefficient-flow coefficient relation and the flow coefficient-speed relation. Later considerations, particularly hi T_2 stator schedules, favored a somewhat different approach. This approach was to employ the use of a throttle coefficient, as a function of flow and design pressure ratio. Throttle coefficient, can be explained as follows: consider a compressor component operating with an atmospheric inlet and an isentropic discharge nozzle which expands back to ambient. The variation of the nozzle throat area required to maintain the compressor on its minimum loss line, relative to the nozzle throat area at design condition, is the throttle coefficient. The throttle coefficient employed is shown in Figure 14. A linear interpolation is used at intermediate pressure ratio. The work coefficient-

speed relations is then derived from the throttle coefficient-flow relation and the flow coefficient-speed relation.

The minimum loss-speed relations are again not convenient. In their place an efficiency ratio flow relation is used. The efficiency ratio is the ratio of efficiency to peak efficiency. This is shown in Figure 15. Also employed is the design point efficiency-pressure ratio relation shown in Figure 16. This completed the definition of the map along the minimum loss line. The loss variation and pseudo-Mach number variation, related to flow, along the speed lines are observed to be linear in nature. Advantage is taken of this linearity to specify these variations as slopes and intercepts. In the case of the loss variation, the curves go through the origin by definition which automatically give the intercept. The slope of the loss variation is shown in Figure 17. On the stall side of the compressor map the Figure 17 loss slope is divided by the minimum loss work coefficient at design point. The slope and intercept of the pseudo-Mach number relation is shown in Figures 18 and 19, respectively. The loss and pseudo-Mach number variations which result for a typical pressure ratio are shown in Figures 20 and 21, respectively.

For high T_2 stator schedules a modification is made to the flow coefficient-speed according to Figure 22. A 45° line on Figure 22 results in the hi T_2 schedule being identical to the low T_2 schedule. A linear interpolation between these two lines is available, so that intermediate stator schedules can be generated. All other input remains unchanged. In this manner the minimum loss line on the map is independent of stator schedule, as are the efficiency characteristics, since both of these are functions of flow only. The flow-speed relation for the high T_2 stator schedule is shown in Figure 23.

A typical map which results from this procedure but for the low T_2 schedule was presented in Figure 1.

ORIGINAL PAGE IS
OF POOR QUALITY

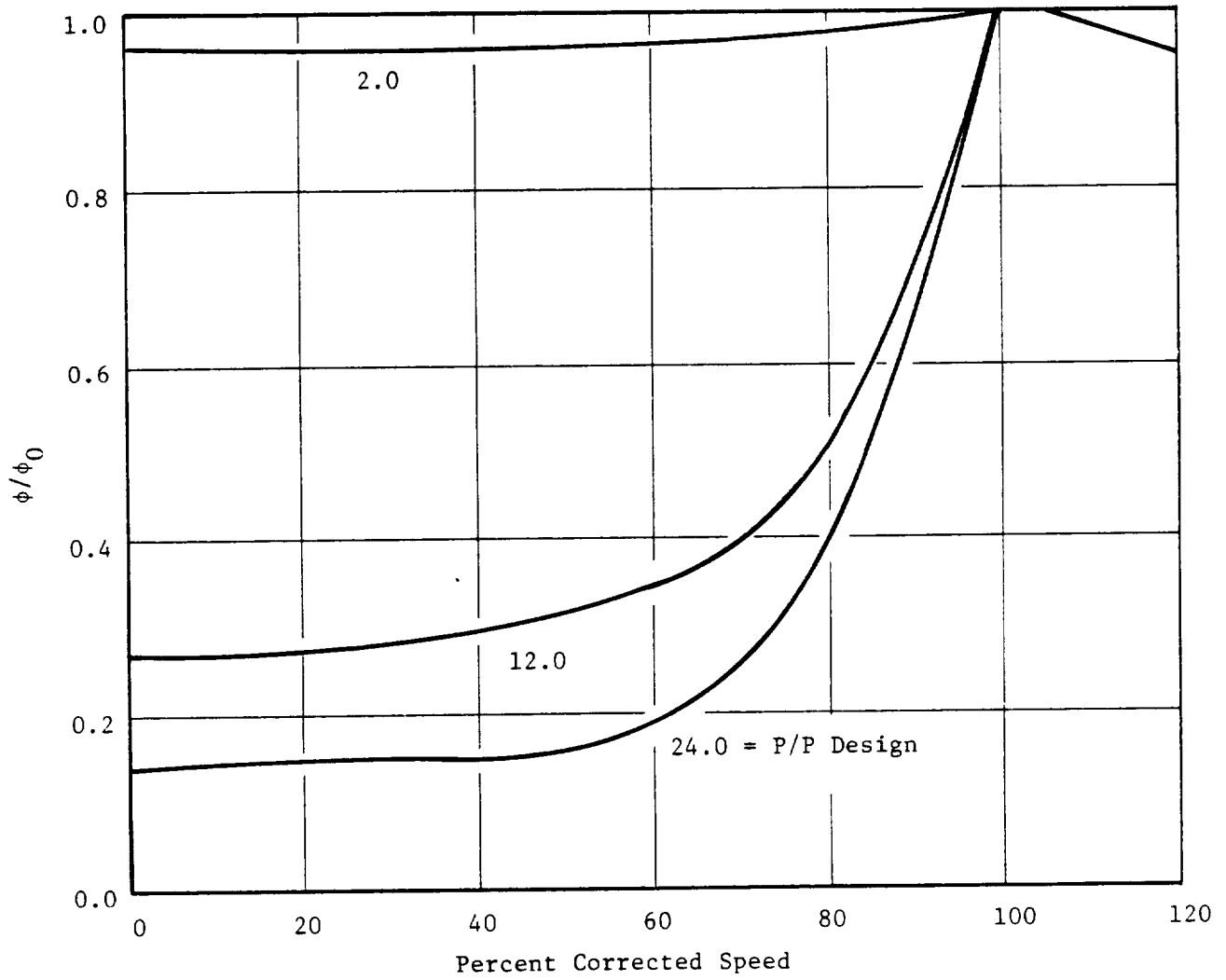


Figure 12. Normalized Flow Coefficient Variation with Speed and Pressure Ratio.

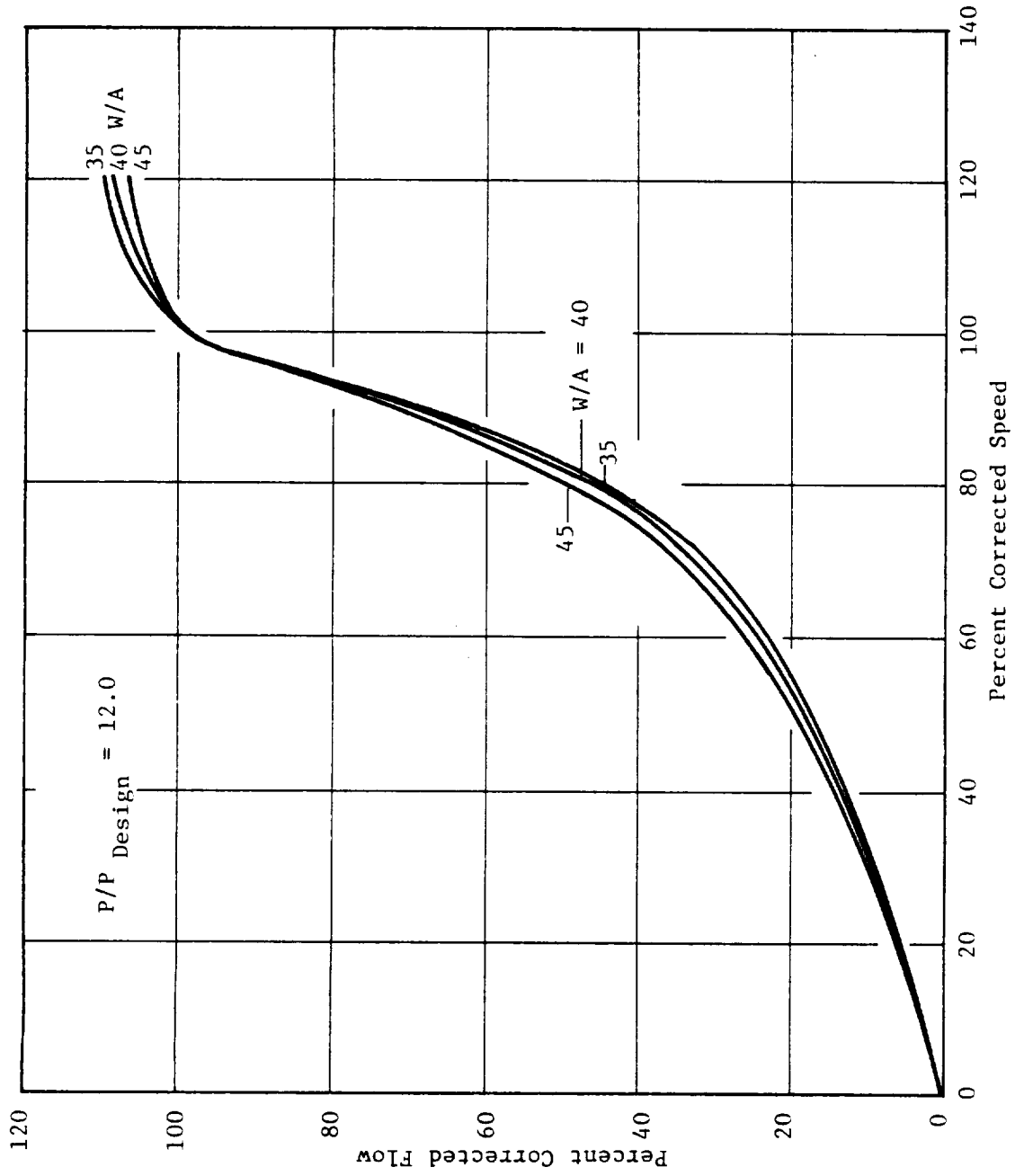


Figure 13. Effect of Specified Flow on Backbone Flow-Speed Relationship.

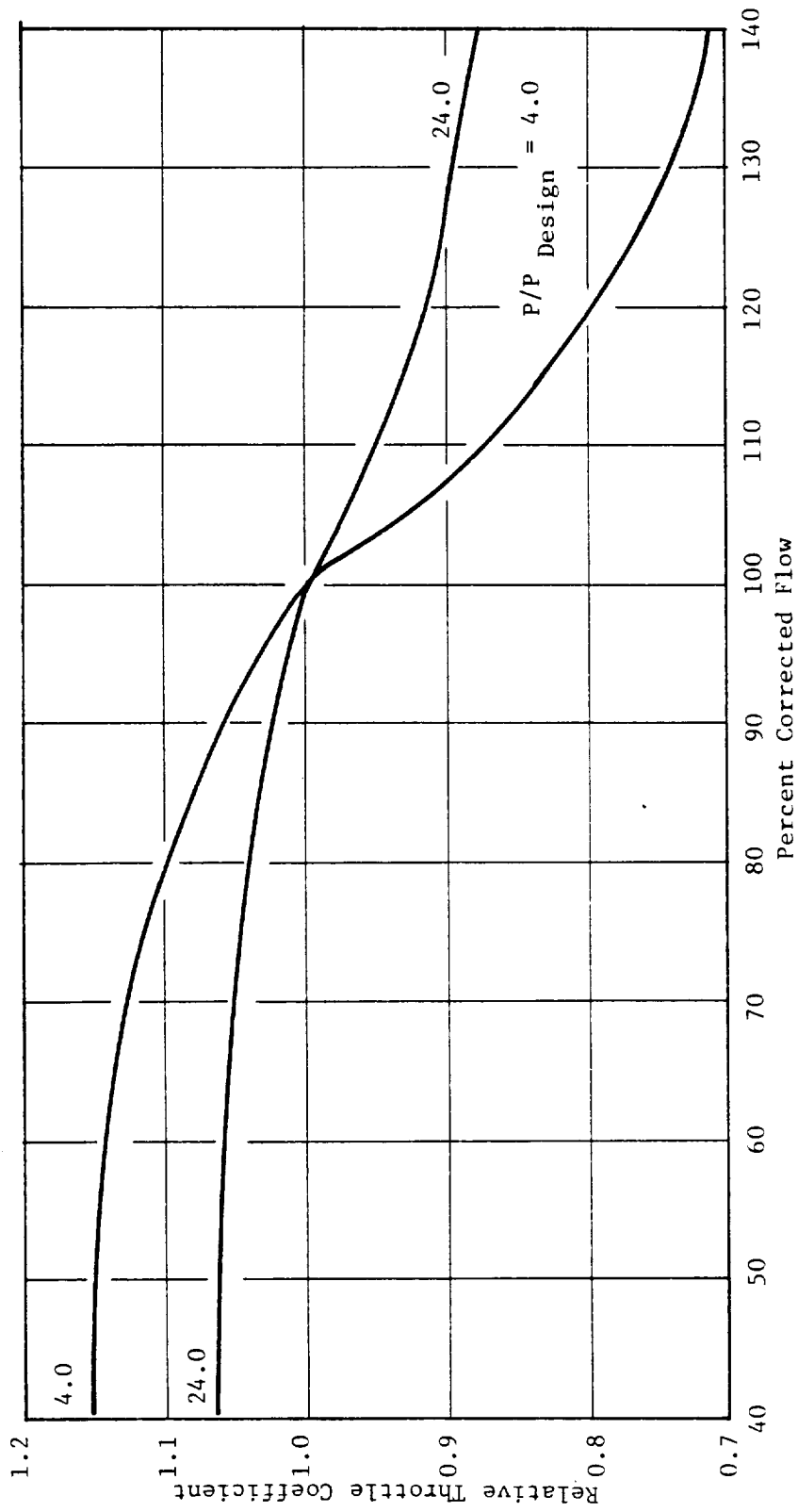


Figure 14. Minimum Loss Throttle Coefficient.

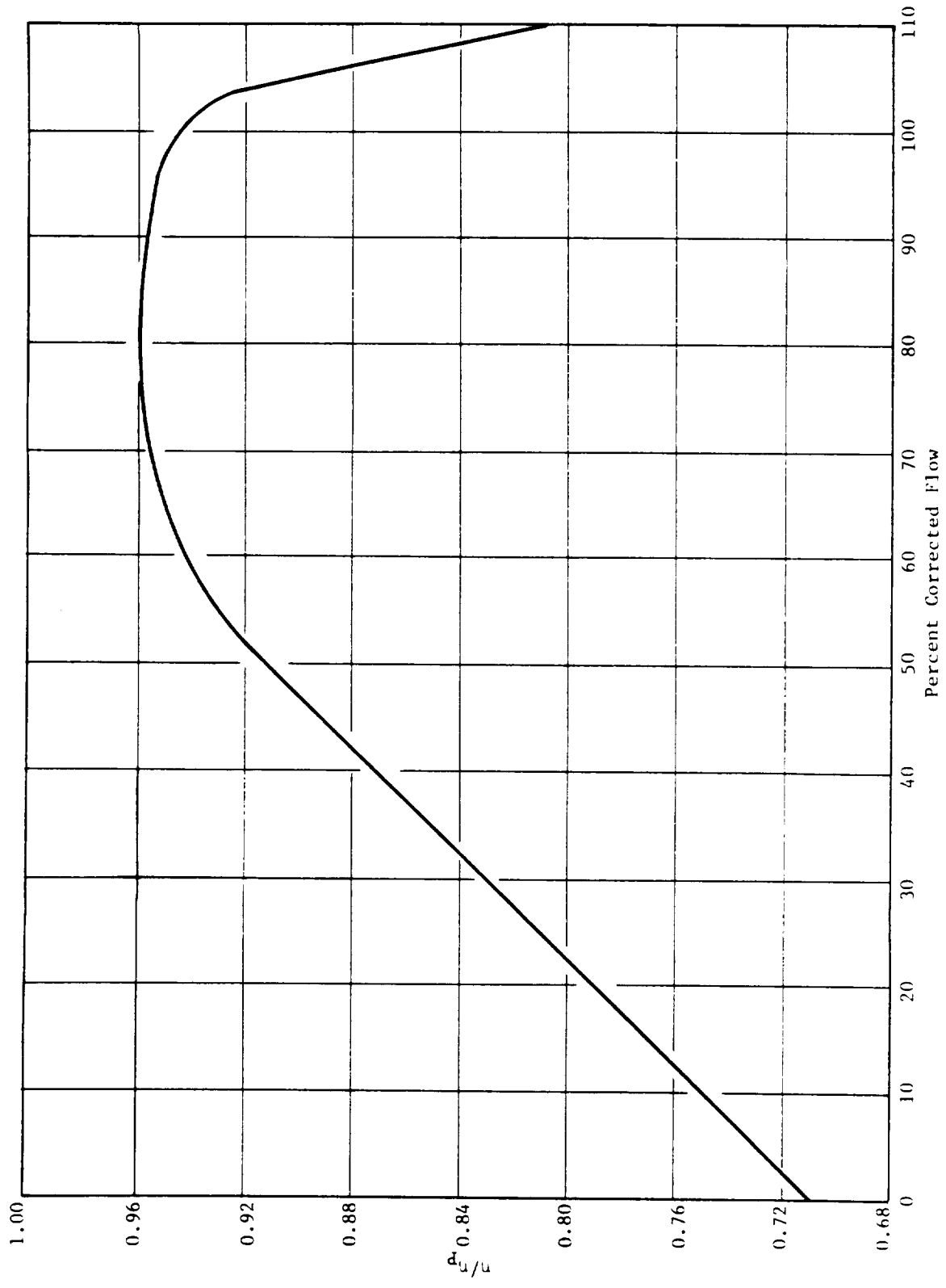


Figure 15. Normalized Minimum Loss Efficiency Distribution.

ORIGINAL PAGE IS
OF POOR QUALITY

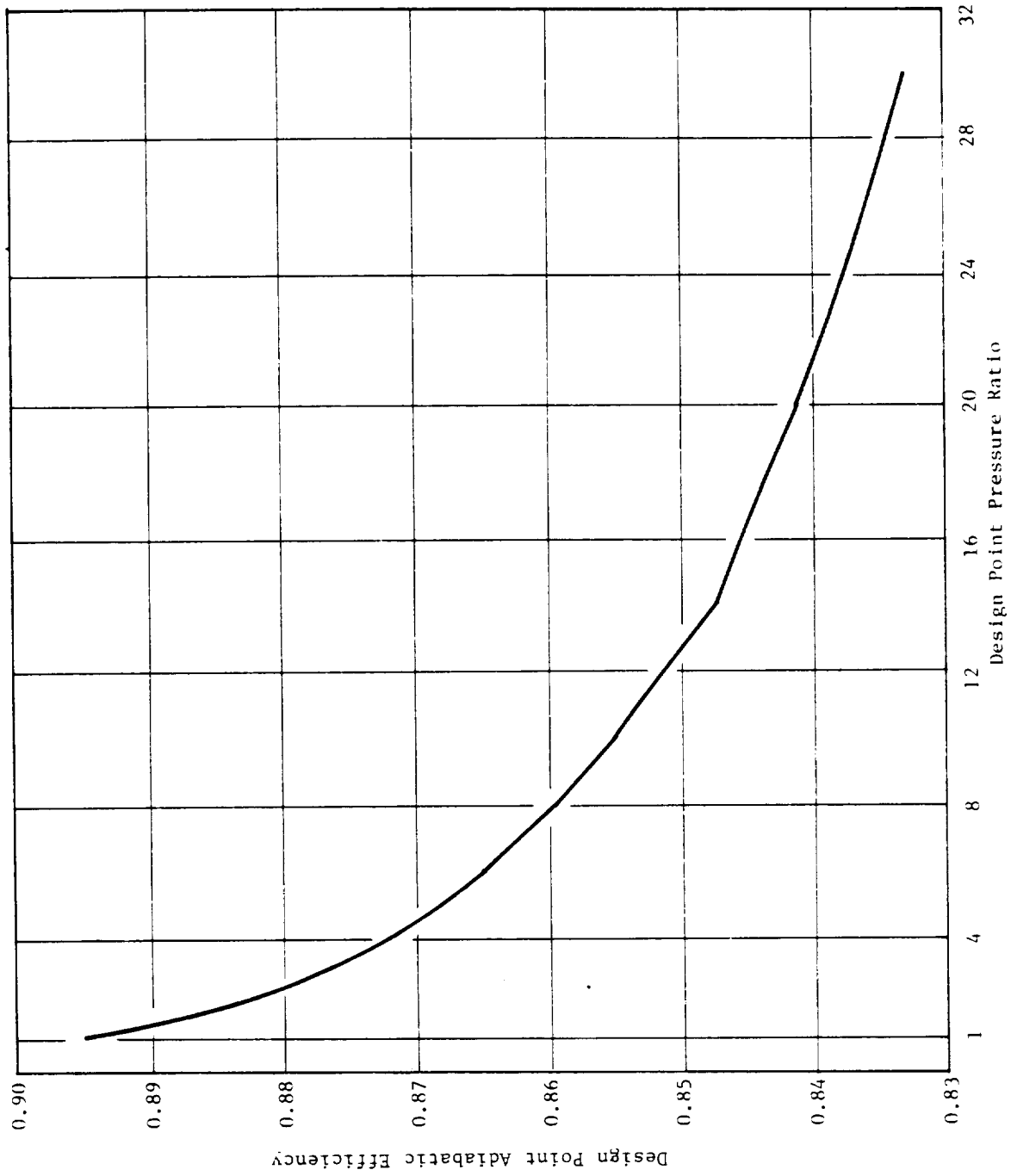


Figure 16. Variation of Design Point Efficiency with Pressure Ratio.

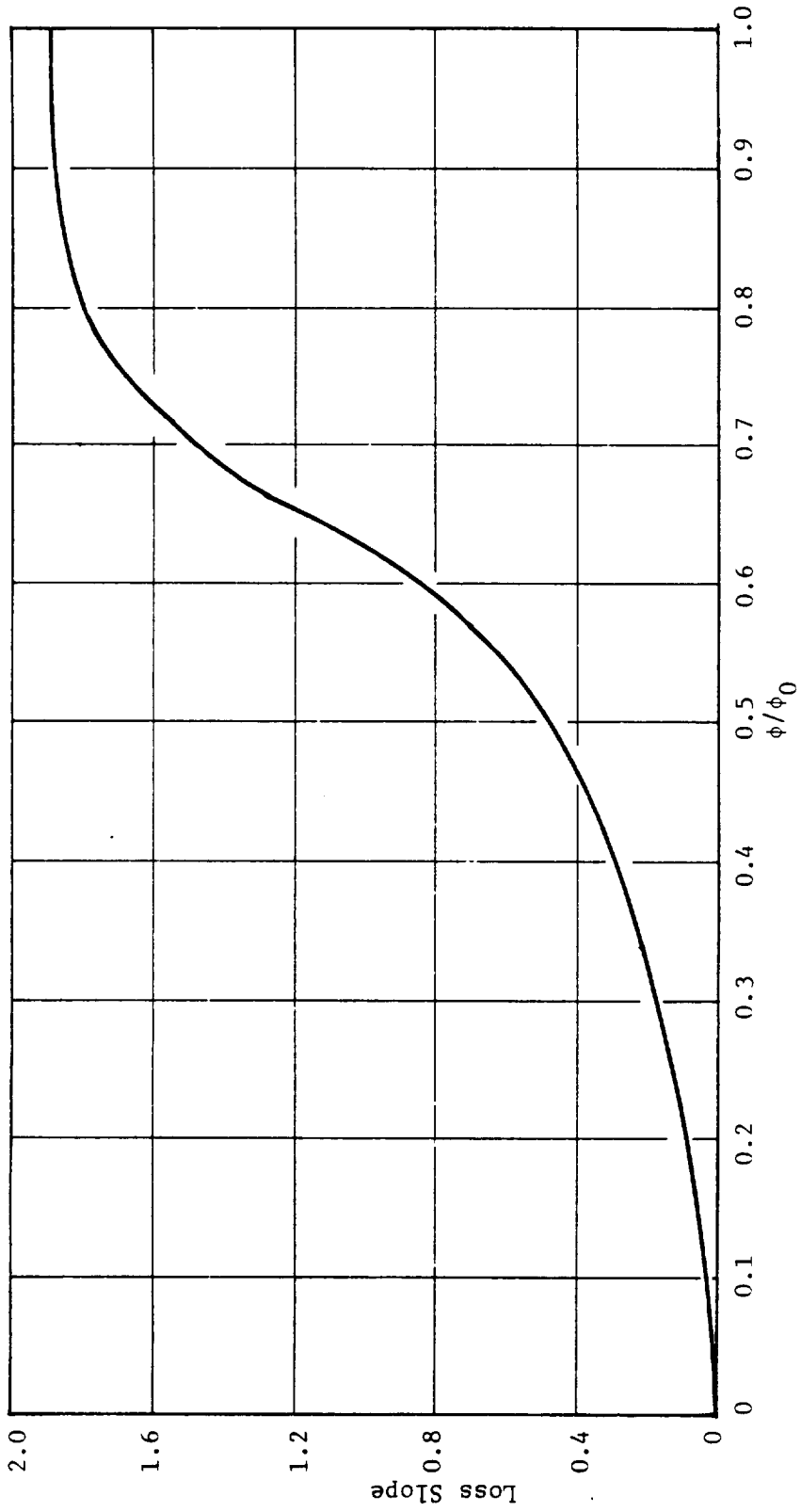


Figure 17. Variation of Loss Slope with Normalized Flow Coefficient.

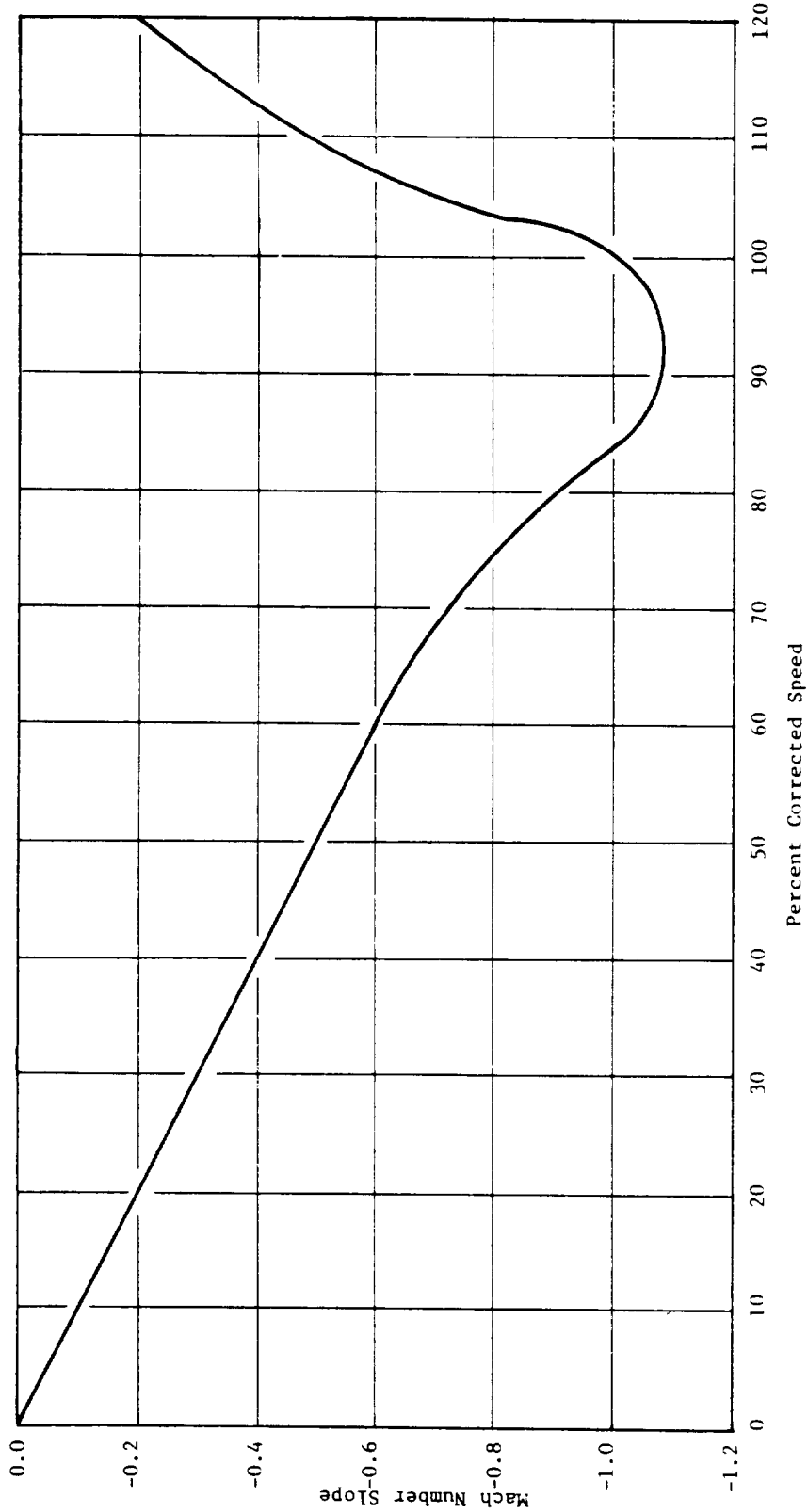


Figure 18. Variation of Mach Number Slope with Speed.

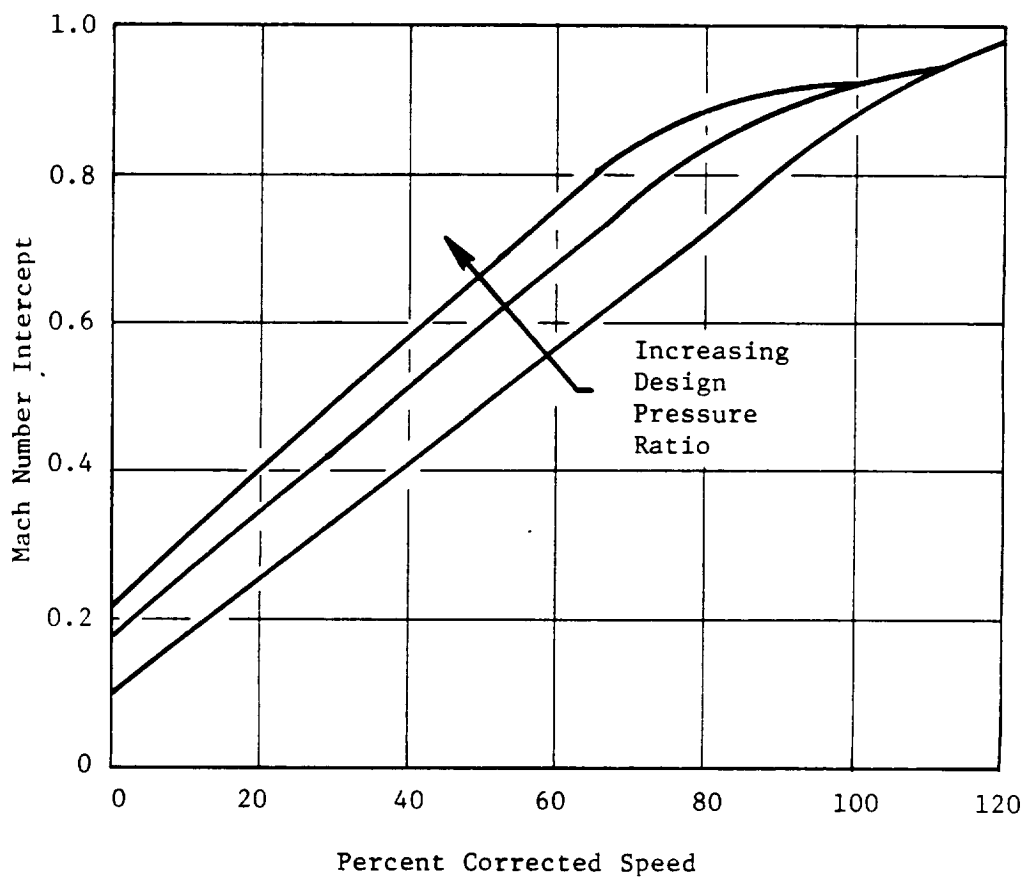


Figure 19. Variation of Mach Number Intercept with Speed and Design Pressure Ratio.

ORIGINAL PAGE IS
OF POOR QUALITY

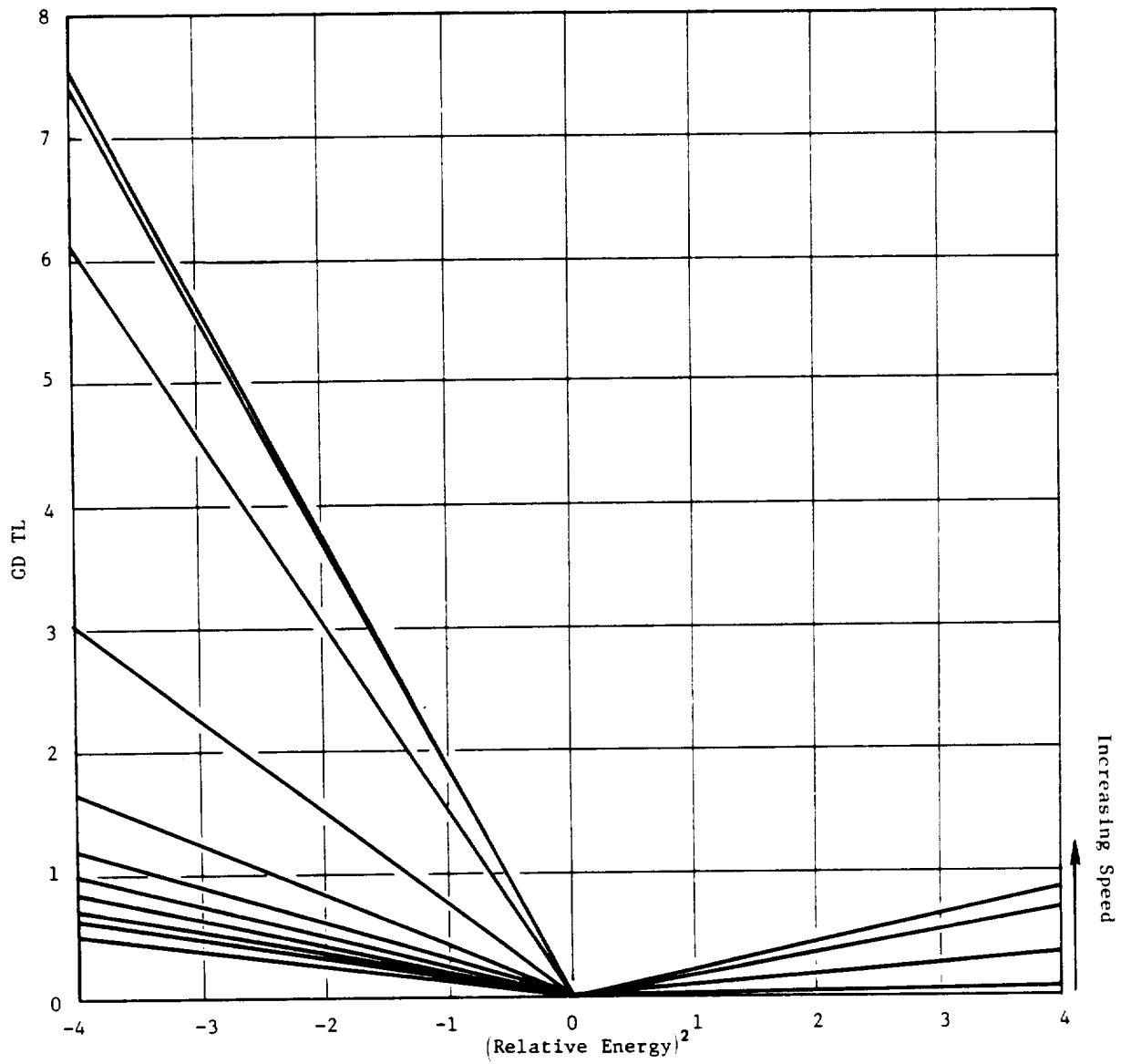


Figure 20. Bivariant Loss Curves.

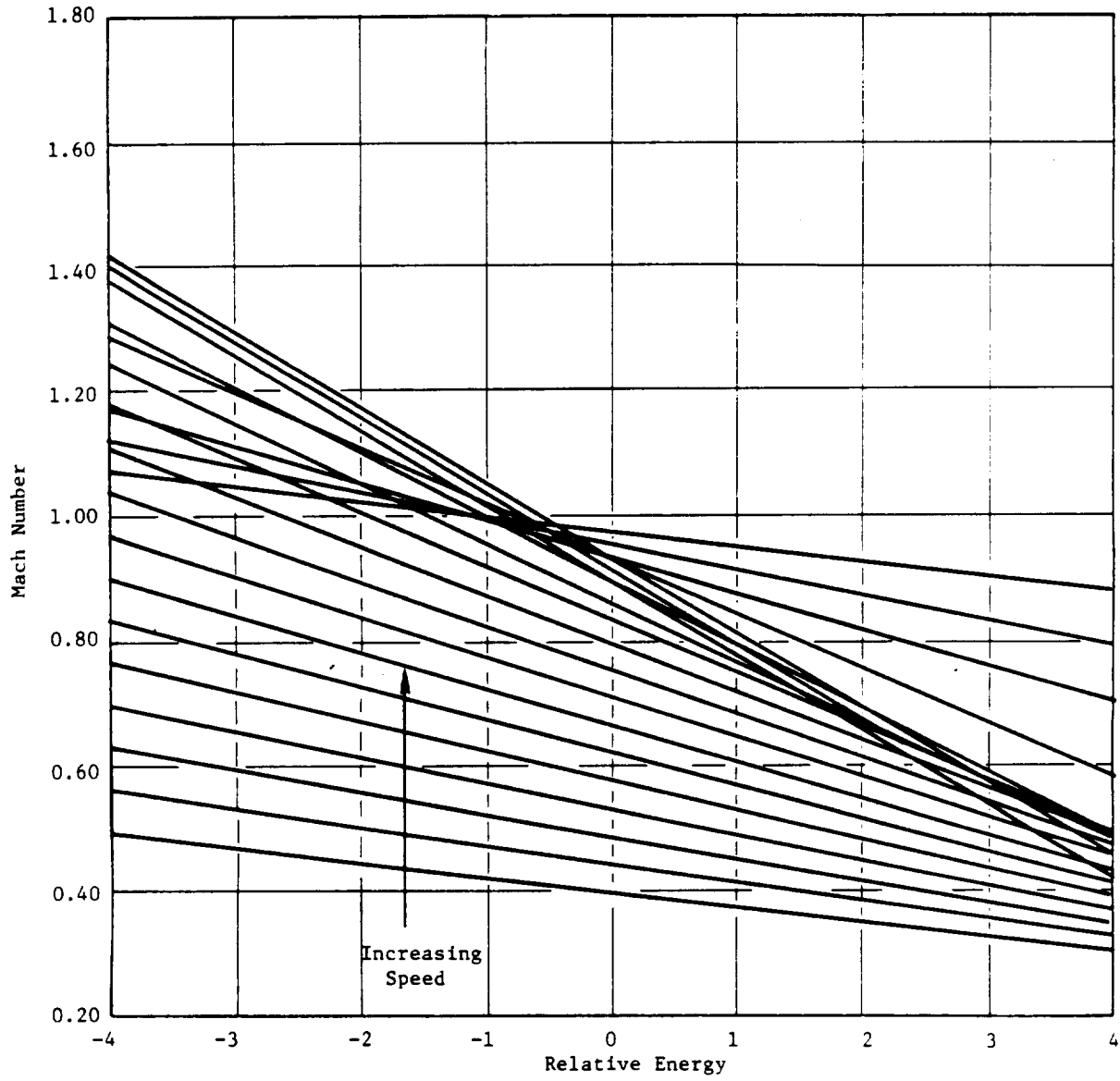


Figure 21. Bivariant Flow Curves.

ORIGINAL PAGE IS
OF POOR QUALITY

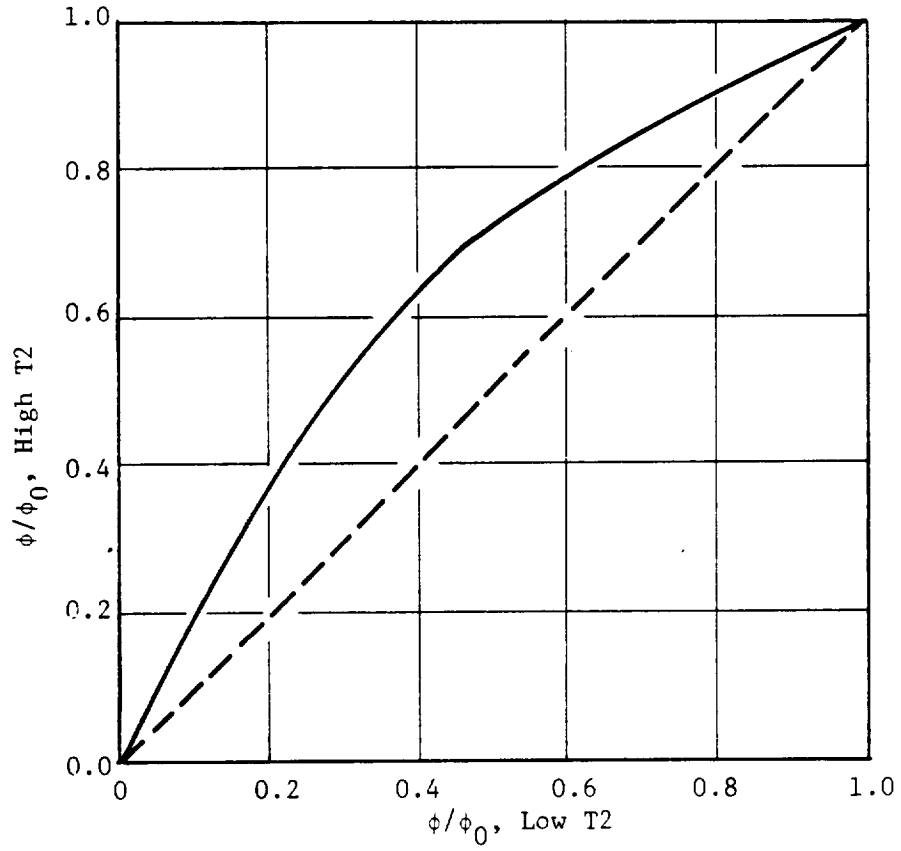


Figure 22. Flow Variation for High T2 Schedule.

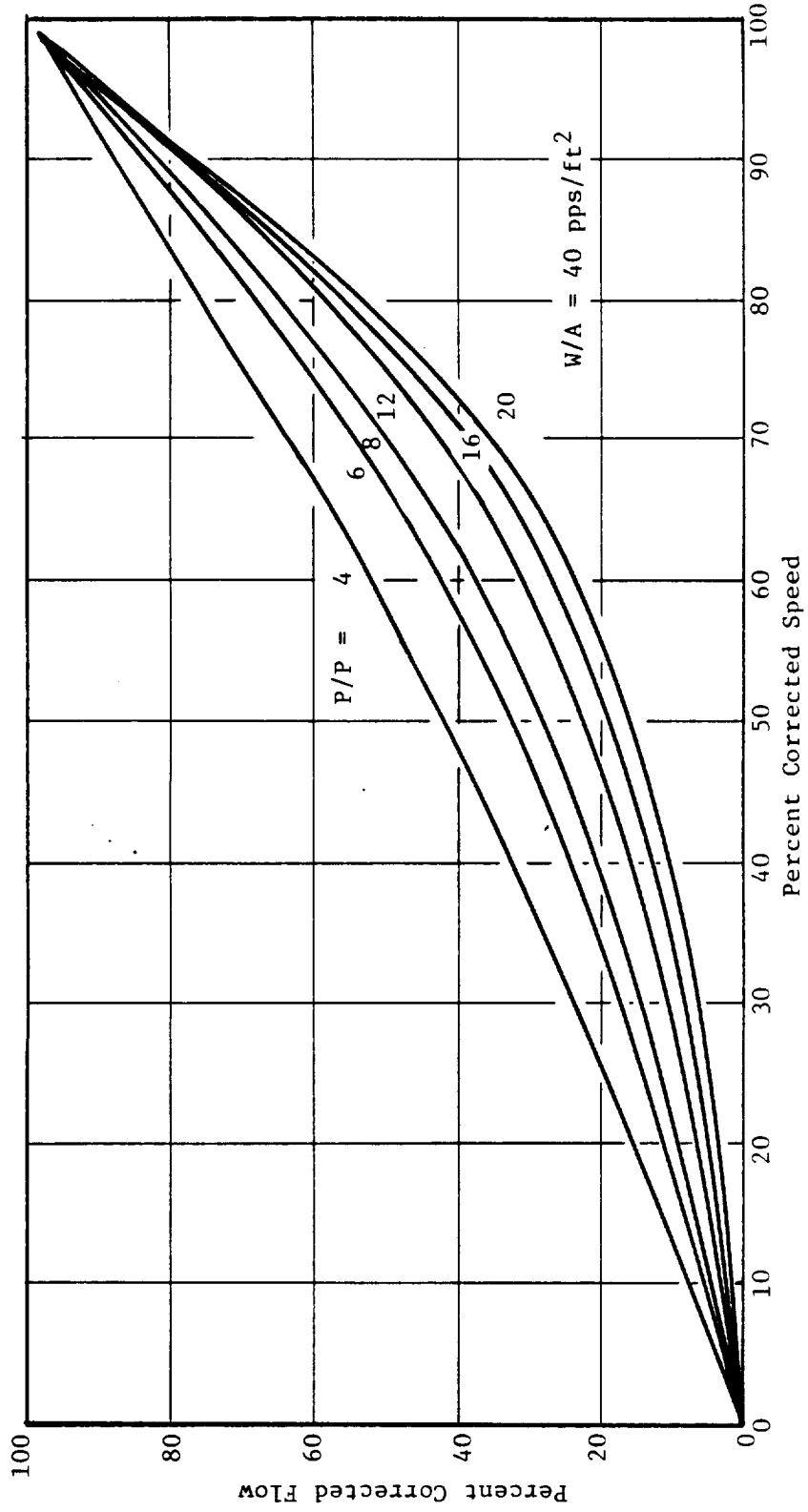


Figure 23. Parametric Map Flow-Speed Relationships HI T2 Schedule.

LIST OF SYMBOLS

A_T	Speed of Sound at Stagnation Temp. fps
A_{ANN1}	Inlet Annulus Area, ft ²
P	Pressure, psia
C	Velocity, fps
T	Temperature, ° C
U	Wheel Speed, fps
W_{corr}	Corrected flow, pps.

α	Stator exit angle
β	Rotor relative angle
ΔH	Change in total enthalpy, Btu/lbm
ρ	Density, lbm/ft ³
ψ	Work Coefficient, $\psi = \Delta H / (U^2 / 2g_c)$
ϕ	Flow Coefficient, $\phi = \dot{Q} / U$

Subscripts

1	Rotor inlet
2	Rotor exit
Design	Design Point
ML	Min-loss point
Std.	Refers to standard day conditions

REFERENCES

1. Fishbach, Laurence H., and Caddy, Michael J., "NNEP: The Navy-NASA Engine Program," NASA TM X-71857, 1975.
2. Fishbach, Laurence H., "Konfig and Rekonfig - Two Interactive Pre-processing Programs to the NAVY/NASA Engine Program (NNEP)," NASA TMX-82636, May 1981.

DISTRIBUTION LIST - FINAL REPORTS - NAS3-23055

NASA Lewis Research Center
 21000 Brookpark Road
 Cleveland, OH 44135

Attn:	Mail Stop	No. of Copies
Report Control Office	60-1	1
Library	60-3	3
M. J. Hartmann	3-7	1
L. W. Schopen	500-305	1
H. Mark	501-12	1
D. N. Bowditch	86-1	1
D. L. Nored	301-2	1
L. D. Nichols	60-2	1
C. L. Ball	60-5	2
L. E. Macioce	6-8	1
H. E. Rohlik	6-10	2
L. H. Fishbach	501-10	25
NASA Scientific and Technical Information Facility P.O. Box 875 Baltimore/Washington International Airport, MD 21240 Attn: Accessioning Department		25

DISTRIBUTION LIST (CONT'D)

One copy each to the following.

Mr. E. G. Blevins
AFWAL/POTA
Wright-Patterson AFB, OH 45433

Ms. Bobbye Ross
AiResearch Manufacturing
Company of Arizona
P.O. Box 5217
Phoenix, AZ 85010

Mr. Len Levine
AVCO-Lycoming Division
550 South Main Street
Stratford, CT 06497

Mr. Dushyant R. Arab
Senior Engineer
Propulsion - R&D
Beech Aircraft Corporation
Wichita, KS 67201

Mr. Erol Onat
The Boeing Company
P.O. Box 3999
Seattle, WA 98124

Mr. Paul W. Reisdorf
Technical Center
Caterpillar Tractor Co.
100 N. E. Adams Street
Peoria, IL 61629

Mr. Gerald W. White
Senior Propulsion Systems Analyst
Office of Scientific and Weapons Research
Central Intelligence Agency
Washington, DC 20505

Mr. Richard A. Sulkoske
Supervisor - Preliminary Design
Detroit Diesel Allison
P.O. Box 894
Indianapolis, IN 46206

Mr. Heiner O. Becker
Project Manager
Engineering Systems
Dresser Industries, Inc.
Dresser Computer Services Division
P.O. Box 796369
Dallas, TX 75379

Mr. M. A. Romano
Advanced Products
Fairchild Republic Company
Farmingdale LI, NY 11735

Mr. Lynn Marksberry
Fluidyne
5900 Olson Memorial Highway
Minneapolis, MN 55422

FTD/SDNP
Attn: M. A. Pennucci
Wright-Patterson AFB, OH 45433

Ms. Joyce R. Stinson, Manager
Systems Computations
Building 240G5
General Electric Co.
1000 Western Avenue
Lynn, MA 01910

Mr. Ronald E. Feddersen
Mail Stop C42-05
Grumman Aerospace Corporation
Bethpage, NY 11714

Mr. Ivan C. Oelrich
IDA/STD
1801 N. Beauregard Street
Alexandria, VA 22311

Mr. J. F. Stroud
Lockheed-California Company
Burbank, CA 91520

Mr. John C. Donohoe
Martin Marietta Aerospace
Mail Point 306
Orlando Division
P.O. Office Box 5837
Orlando, FL 32855

Eugene E. Covert, Sc.D.
 Professor and Director
 Department of Aeronautics and Astronautics
 Center for Aerodynamic Studies
 Massachusetts Institute of Technology
 Cambridge, MA 02139

Dr. Robert T. Taussig
 Director of Energy Technology
 Mathematical Sciences North West, Inc.
 2755 Northup Way
 Bellevue, WA 98004

Mr. Donald C. Bingaman
 McDonnell Douglas Corporation
 271/C9A
 P.O. Box 516
 St. Louis, MO 63166

NASA Ames Research Center
 237-11/Tom Galloway
 Moffett Field, CA 94035

National Aeronautics and Space Administration
 George C. Marshall Space Flight Center
 Attn: PD31-78-41
 Marshall Space Flight Center, AL 35812

NASA Langley Research Center
 249/Shelby J. Morris
 Hampton, VA 23665

Mr. Michael Caddy
 Code 6052
 Naval Air Development Center
 Warminster, PA 18974

Mr. Paul Piscopo
 Naval Air Propulsion Center
 P.O. Box 7176
 Trenton, NJ 08628

F. J. O'Brimski, Commander
 Naval Air Systems Command
 AIR-5284C2/JEL
 Department of the Navy
 Washington, DC 20361

Professor Thomas Houlihan
 Code 69 HM
 Naval Post Graduate School
 Monterey, CA 93940

56

Mr. Andre By
 Northern Research and Engineering Company
 39 Olympia Avenue
 Woburn, MA 01801

Mr. Arif Dhanidina, 3813/82
 Propulsion Research
 Northrop Aircraft Division
 One Northrop Avenue
 Hawthorn, CA 90250

Mr. Douglas Lee, 3828/52
 Advanced Propulsion/Thermal Analysis
 Northrop Aircraft Division
 One Northrop Avenue
 Hawthorn, CA 90250

Mr. Henry Snyder
 Pratt & Whitney Aircraft Group
 Engineering Computer Applications
 Government Products Division, M/S 712-28
 P.O. Box 2691
 West Palm Beach, FL 33402

Mr. Robert Howlett
 Pratt & Whitney Aircraft Division
 400 Main Street
 Mail Stop EB1F1
 East Hartford, CT 06108

Mr. Larry Carroll
 Propulsion Dynamics Inc.
 2200 Somerville Road
 Annapolis, MD 21401

Mr. William E. Flaus-D/71 B/6
 North American Aircraft Division
 Rockwell International
 4300 East Fifth Avenue
 P.O. Box 1259
 Columbus, OH 43216

Mr. Larry Miller
 Aerospace Marketing Manager
 Rosemount Incorporated
 P.O. Box 959
 Burnsville, MN 55337

Mr. Nate Anderson
 Mail Zone E-9
 Solar Turbines International
 P.O. Box 80966
 San Diego, CA 92138

Professor I-Dee Chang
 Department of Aeronautics and Astronautics
 William F. Durand Building
 Stanford University
 Stanford, CA 94305

Mr. Gerald J. Herman
 Williams Research Corporation
 2280 West Maple Road
 Walled Lake, MI 48088

Mr. Mark A. Chappell
 Sverdrup Technology Inc.
 Mail Stop 500
 Arnold Air Force Station, TN 37389

Mr. John J. Fox
 Teledyne CAE
 1330 Laskey Road
 P.O. Box 6971
 Toledo, OH 43612

Commander
 US Army Aviation Research & Development
 Command
 Attn: DRDAV-DP/Dennis Enders
 4300 Goodfellow Blvd.
 St. Louis, MO 63120

Mr. Mike Galvis - DAVDL-ATL-ATP
 Applied Technology Laboratory
 U.S. Army Research Laboratory (AAVRADOM)
 Fort Eustis, VA 23604

Dr. Paul C. Glance
 Chief, Engine Function
 Department of The Army
 U.S. Army Tank-Automotive Research
 and Development Command
 Warren, MI 48090

Dr. Walter O'Brien
 Mechanical Engineering Dept.
 Virginia Polytechnic Institute
 Blacksburg, VA 24061

Dr. Reginald G. Mitchiner
 Associate Professor of Mechanical Engineering
 Virginia Polytechnic Institute and State
 Univ.
 Blacksburg, VA 24061

Mr. W. M. Rhoades
 Manager, Propulsion and Thermodynamics
 Vought Corporation
 P.O. Box 225907
 Dallas, TX 75265

